Sworn statement

I hereby declare that I am the sole author of this thesis and have written it without the help of third parties. Ideas and quotations from other sources that I used directly or indirectly are marked. This thesis has not yet been presented to an examination office and has not yet been published.

Eidesstattliche Erklärung

Hiermit versichere ich an Eides statt, die vorligende Arbeit selbständig und ohne Hilfe Dritter angefertigt zu haben. Gedanken und Zitate, die ich aus fremden Quellen direkt oder indirekt übernommen habe, sind als solche kenntlich gemacht. Diese Arbeit hat in gleicher oder ähnlicher Form noch keiner Prüfungsbehörde worgelegen und wurde bisher nicht veröffentlicht.

Berlin, September the 4th, 2017

José María Subías Rapún

Abstract

Adsorption onto Granular Ferric Hydroxide (GFH), a commercially available, synthetic adsorbent is a well-known technique used in water treatment for the purification of water. For this study, a fine fraction of granular ferric hydroxide (< 0.3 mm) was used as adsorbent for removal of phosphorus and chromium species. Effects of changing contact time, pH, water matrix and concentration of adsorbate were determined for different amounts of granular ferric hydroxide.

Adsorption of phosphate was studied in batch experiments. Equilibrium isotherms show that adsorption of phosphate is pH and water matrix dependent. High adsorbent loadings up to 24 mg/g P for the equilibrium concentration of 2 mg/L P (at pH 6 in Deionized water (DI)) and up to 25 mg/g P for the equilibrium concentration of 3 mg/L P (at pH 7 in Berlin Drinking water (DW)) were achieved. The presence of calcium could be the reason of a more efficient adsorption in DW compared to DI water. For the same water matrix, higher capacities were reached for lower pH, in the analyzed range from 6 to 8. Presence of NaCl in DI water is shown to improve the adsorption of phosphate, but not very significantly.

Adsorption of chromium onto the fine fraction of granular ferric hydroxide did not achieve such a high capacity in comparison to phosphate. Equilibrium isotherms show the influence of pH and water matrix on the adsorption. Adsorption at pH 6 can reach higher capacities (7.56 mg/g Cr) compared to a higher pH value (2.97 mg/g Cr at pH 8). Adsorption of chromium in DW shows very low capacity values compared to the other cases. The maximum adsorbent loading achieved was 1.65 mg/g Cr for an equilibrium concentration of 3 mg/L Cr. Concentration of sulfate ions in Berlin DW could compete with chromium in the interaction with GFH. The interfering effect could be a reason of a less efficient chromium adsorption. Presence of other competing ions like chloride or silicates could also affect the process.

As a second part of this study, iron oxyhydroxide agglomerates were used as adsorbent for phosphate and chromate species. Under same conditions of pH and water matrix, adsorption onto agglomerates presents less strong adsorption, the maximum capacity values were 6.4 mg/g for Cr and 3.2 mg/g for P. However, the sources consulted show similar adsorbent loadings achieved for chromium adsorption, compared to GFH adsorption (27 mg/g Cr as maximum adsorbent loading achieved).

CONTENTS

1. Introduction

Phosphorus is an essential nutrient for all living organisms. However if phosphate levels are too high in bodies of water such as lakes or rivers, eutrophication can result. Phosphate normally enters the affected surface water as a result of agricultural run-off from fertilized fields or sewage effluent discharge (Rabah, 2015).

Chromium, priority metal pollutant, exists primarily in trivalent and hexavalent states in the aquatic environment. The trivalent chromium is relatively non-toxic and in fact an essential trace nutrient in the human diet, but the hexavalent chromium is very toxic, being a mutagen and a potential carcinogen (Asgari *et al.*, 2008).

In this study, phosphate and chromium adsorption onto Granular Ferric Hydroxide (GFH), a commercially available ferric hydroxide adsorbent used in fixed-bed water treatment systems, is analyzed. GFH was developed between 1990 and 1994 by the department of Water Quality Control of Berlin Institute of Technology and produced since 1997 by the company GFH Wasserchemie (Osnabrück, Germany) (Sperlich, 2010).

The experiments were performed using a fine fraction of GFH, being resource-efficient, as it would be wasted if no use is found. The predicted kinetics are better for the fine fraction of GFH.

Chapter 2 shows a literature review of general adsorption process and adsorption onto granular ferric hydroxide. Available literature on phosphorus and chromium is reviewed, in terms of chemistry, occurrence and environmental impacts.

Chapter 3 describes the used material and followed method to perform the experiments, providing all the needed information to accomplish the process.

Results are shown in chapter 4. Equilibrium isotherms of phosphate and chromium are analyzed for different conditions of pH and water matrix.

1.1. Objective

The main objective of the study is to develop equilibrium isotherms for the adsorption of phosphorus and chromium species onto the fine fraction of granular ferric hydroxide with different conditions and analyze the adsorbent loading that can be achieved for different pH values and water matrixes.

A second objective is to compare the results of the adsorption onto the fine fraction of GFH with conventional granular ferric hydroxide adsorbents and analyze possible sources of error in performed experiments.

2. Literature review

2.1. Chromium

Chromium and its ions have intensive use in different industries. The environmental consequences are considerable. Therefore chromium removal from wastewater and ground water or modification of the structure of the ions to the non-toxic form has a significant importance (Zelmanov and Semiat, 2011).

Polluted water and process waste streams from mining operations, metal-plating facilities, power generation facilities, electronic device manufacturing units and tanneries often contain chromium such as trivalent and hexavalent chromium ions at concentrations above local discharge limits (Zelmanov and Semiat, 2011).

Chromium, priority metal pollutant, exists primarily in trivalent and hexavalent states in aquatic environment. The trivalent chromium is relatively non-toxic and in fact an essential trace nutrient in the human diet, but the hexavalent chromium is very toxic, being a mutagen and a potential carcinogen. Hexavalent chromium, which is primarily present in two forms of chromate (CrO_4^{2-}) and dichromate ($Cr_2O_7^{2-}$), poses significantly higher levels of toxicity in comparison with other valence states (Asgari *et al.*, 2008).

According to EU and WHO standards the maximum total chromium content in drinking water is 0.05 ppm. There is no universal method for the chromium removal from water. A variety of possible methods of chromium removal treatment from industrial wastewater and ground water are known: chemical precipitation, reduction, extraction, adsorption, ion exchange, and reverse osmosis. These processes have some inconvenience and limits due to high energy requirements, a large amount of the produced sludge and incomplete chromium removal (Zelmanov and Semiat, 2011).

2.2. Phosphorus

Phosphorus (P), having the atomic number 15 and an atomic weight 0f 30.97 is he eleventh most abundant element in the earth's crust and widely present in rocks, soils, waters and in living organisms (Sperlich, 2010).

Phosphorus is the eleventh most abundant element in the Earth´s crust, widely present in rocks, soils, water and living organisms. Phosphorous is essential in living processes, forming the backbone of DNA and participating in metabolic energy transfer (Sperlich, 2010).

Phosphorus in its natural state, is combined with four oxygen molecules, resulting in a phosphate oxyanion. There is a big amount of phosphorous compounds associated with oxygen, carbon, nitrogen and metals (Sperlich, 2010).

The main sources of phosphorous in wastewater originate from human excreta and, in

some countries, from the use of detergents. The pollution by phosphate in water is the main reason of eutrophication, dangerous for the sustainability of the aquatic life, caused by the reduction of dissolved oxygen and harmful algae blooms (Sperlich, 2010).

In natural and waste water, phosphorus is dispersed between different physical compartments such as dissolved and colloidal fractions, humic and fulvic acids or biological constituents in aquatic organisms. The measured fractions are not identical to the established specific chemical or physical components (Sperlich, 2010).

Studying the most common pH range in natural waters (pH 6-9,5) it is possible to observe that the dominant species forms of phosphorous are $H_2PO_4^-$ (monovalent) and HPO_4^{2-} (divalent), after the dissociation of phosphoric acid (Sperlich, 2010).

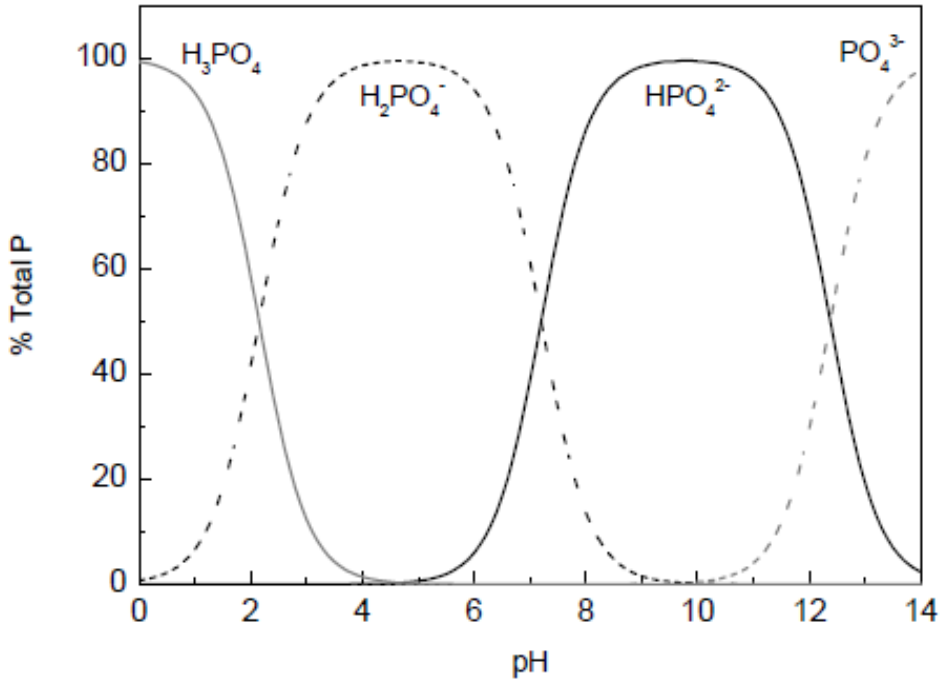

Figure 2.1: Aqueous speciation of phosphoric acid as pH function (Sperlich, 2010).

Phosphorus removal has become more widely employed in wastewater treatment and emissions of phosphorus from sewage into surface waters, across Europe, have typically fallen by 30-60 % since the mid-1980's, with considerable variations across the continent. Similar control measures have been implemented in the U.S.A. and Japan. E.g., the U.S. EPA has established a maximum contaminant level for phosphorus to be < 20 µg/L in rivers and streams and in lakes and reservoirs during summer growing season (Sperlich, 2010).

There is no universal technique for the phosphate removal from water. Physicochemical techniques are usually used for the phosphate removal from municipal and industrial wastewater beside biological nutrient removal methods. The most widely applied

activated sludge biological wastewater treatment process achieves a removal of only 75–85% of total phosphate. Physicochemical and biological treatment methods mostly transfer phosphate from the liquid to the sludge phase, which required transportation and disposal elsewhere (Zelmanov and Semiat, 2015).

2.3. Adsorption

The most general definition describes adsorption as an enrichment of chemical species from a fluid phase on the surface of a liquid or a solid. In adsorption theory, the solid material that provides the surface for adsorption is referred to as adsorbent; the species that will be adsorbed is named adsorbate. By changing the properties of the liquid phase, adsorbed species can be released from the surface and transferred back into the liquid phase in a reverse process referred to as desorption (Worch, 2014)**.**

This process creates a film of the adsorbate on the surface of the adsorbent. This process differs from absorption, in which a fluid (the absorbate) is dissolved by or permeates a liquid or solid (the absorbent), respectively. Since adsorption is a surface process, the surface area is a key quality parameter of adsorbents. The adsorbents are typically highly porous materials. Their porosity results in large surfaces as internal surfaces constituted by the pore walls (Worch, 2014).

Adsorption is a phase transfer process that is widely used in practice to remove substances from fluid phases (gases or liquids). It can also be observed as a natural process in different environmental compartments. In water treatment, adsorption has been proved as an efficient removal process for a multiplicity of solutes. Here, molecules or ions are removed from the aqueous solution by adsorption onto solid surfaces (Worch, 2014).

The practice-oriented adsorption theory consists of three main elements: adsorption equilibrium, adsorption kinetics and adsorption dynamics.

Adsorption equilibrium

The dependence of the adsorbed amount on the adsorbate concentration and temperature is described by the adsorption equilibrium, being the general form to define it:

$$q_{eq} = f(c_{eq}, T) \tag{2.1}$$

q_{eq} : adsorbed concentration

c_{eq} : equilibrium adsorbate concentration

T: temperature

The equilibrium is considered at constant temperature, in the form of an adsorption

isotherm, that serves to describe the equilibrium at a constant temperature through experimental models, as it is shown in figure 2.2. It is common to keep it constant in practice, for a matter of simplification, being then the. general form:

$$q_{eq} = f(c_{eq}) \; ; \quad T = const \tag{2.2}$$

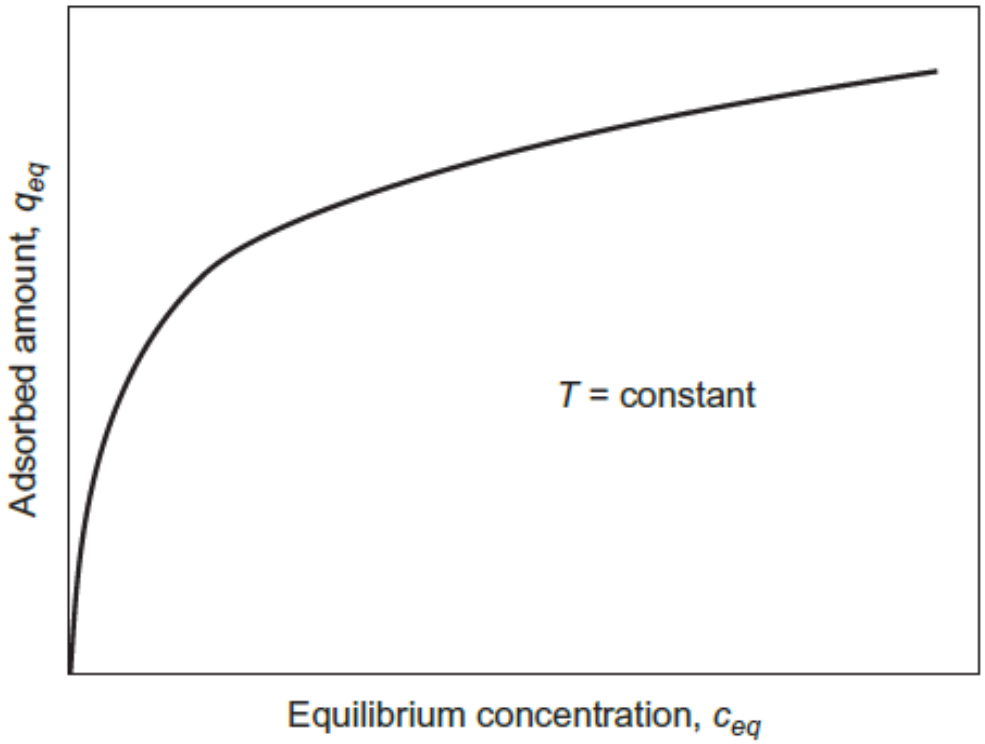

Figure 2.2: Adsorption isotherm (Worch, 2014).

The adsorbed amount at the equilibrium concentration is usually represented by an isotherm at constant temperature, obtained by regression analysis. All the measured numeric data obtained experimentally are described with a corresponding isotherm equation (Worch, 2014).

To determine adsorption equilibrium data, the bottle-point method is usually applied. Inside each bottle there is the known volume of adsorbate solution V_L, with a known initial concentration c_0, in addition to a determined adsorbent mass, m_a. After reaching the equilibrium the equilibrium concentration c_{eq} and the adsorbed amount q_{eq} can be measured and calculated respectively. The relation $\frac{m_a}{V_L}$ is defined as adsorbent dose (Worch, 2014).

Using the material balance equation to obtain the adsorbed amount in equilibrium,

$$V_L * (c_0 - c_{eq}) = m_a * (q_{eq} - q_0) \quad (2.3)$$

and having an initial null adsorbed concentration, finally the balance is reduced to:

$$q_{eq} = \frac{V_L}{m_a} * (c_0 - c_{eq}) \quad (2.4)$$

There are two possibilities to obtain different points for the isotherms:

1) Variation of the adsorbent dose at constant c_0. (Figure 2.3)

2) Variation of c_0 at constant adsorbent dose. (Figure 2.4)

The diagrams show the equilibrium curve together with the operating line. The isotherm points found by one of these methods can be drawn in a diagram, $q_{eq}=f(q_{eq})$, and can also be fitted by using an isotherm equation, that could be derived from theoretical considerations or be empirical (Worch, 2014).

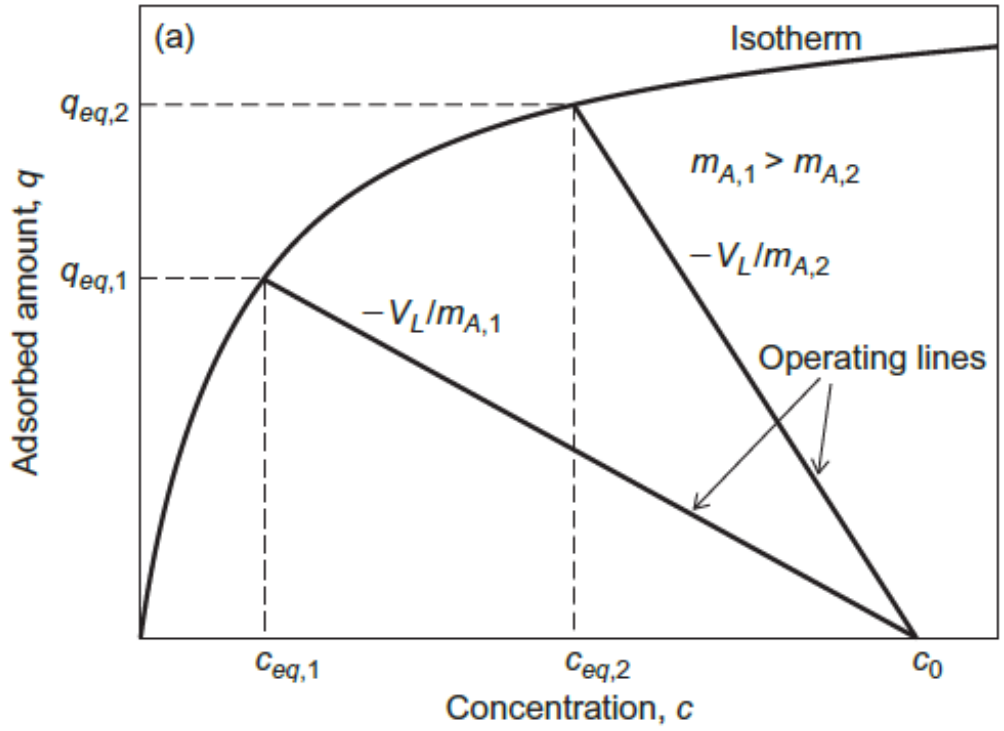

Figure 2.3: Determination of adsorption isotherm by variation of adsorbent dose (Constant c0) (Worch, 2014).

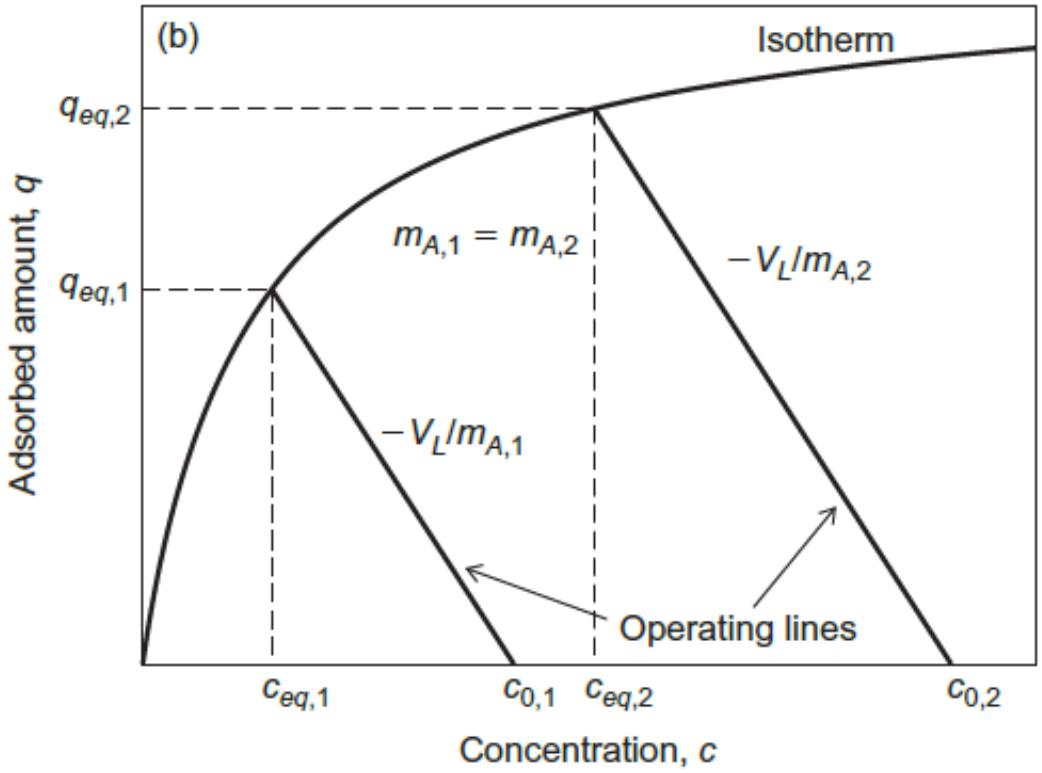

Figure 2.4: Determination of adsorption isotherms by variation of initial concentration (Constant adsorbent dose) (Worch, 2014).

Langmuir and Freundlich isotherm

The use of an isotherm equation that provides the results of the experimental isotherm curves with precision is complicated. For practical application, the most important fact is to find a suitable mathematical equation that grants characterization of the isotherm data as simple as possible (Worch, 2014).

The Langmuir and Freundlich equations have a major significance in the group two-parameter isotherms, due to the fact that they are the most frequently used isotherm equations (Worch, 2014).

The Langmuir adsorption isotherm, used to describe the equilibrium between surface and solution as a reversible chemical equilibrium between species, is given by

$$q^* = q_{max} * \frac{K_L * c^*}{1 + K_L * c^*} \quad (2.5)$$

K_L : Langmuir coefficient

q_{max}: maximum adsorbed concentration

c^*: equilibrium adsorbate concentration

q^*: adsorbed concentration

The Langmuir isotherm is often not suitable to describe the experimental isotherm data found for aqueous solutions, which is a consequence of often not fulfilled assumptions which this theoretically derived isotherm is based on, particularly monolayer coverage of the adsorbent surface and energetic homogeneity of the adsorption sites. (Worch, 2014)

That is why the Langmuir equation is in most cases only applicable for small concentration ranges, since the surface of GFH, for example, is of a heterogeneous nature (Sperlich, 2010).

Parameter q_{max} has the same unit as the adsorbent unit, while K_L is the reciprocal of the concentration unit, indicating a monolayer coverage of the adsorbent surface. To derive the parameters, equation [2.5] can be linearized (Sperlich, 2010).

On the other hand, the Langmuir isotherm equation was also found to be applicable in cases where the underlying assumptions were obviously not fulfilled (Worch, 2014).

The Freundlich isotherm was proposed as an empirical equation for heterogeneous adsorbents, having the form

$$q^* = K_F * c^{*n} \quad (2.6)$$

K_F and n are the isotherm parameters. They have to be obtained in batch experiments by logarithmic regression of the data in the linearized form of the equation (Sperlich, 2010).

The Freundlich isotherm can be linearized by transforming the equation into the logarithmic form

$$logq^* = logK_F + n * logc^* \quad (2.7)$$

or

$$lnq^* = lnK_F + n * lnc^* \quad (2.8)$$

Adsorption coefficient, K_F, characterizes the strength of adsorption. The higher K_F, the higher is the adsorbent loading that can be achieved. Exponent n is related to the energetic heterogeneity of the adsorbent surface, determines the curvature of the isotherm. In practice, mostly n values lower than 1 are found. The lower the n value is, the more concave is the isotherm shape, becoming linear with n=1. Freundlich isotherms with $n < 1$ show relative high adsorbent loadings at low concentrations. Isotherms with $n > 1$ are characterized as unfavorable (Worch, 2014). (See Figure 2.5 and 2.6)

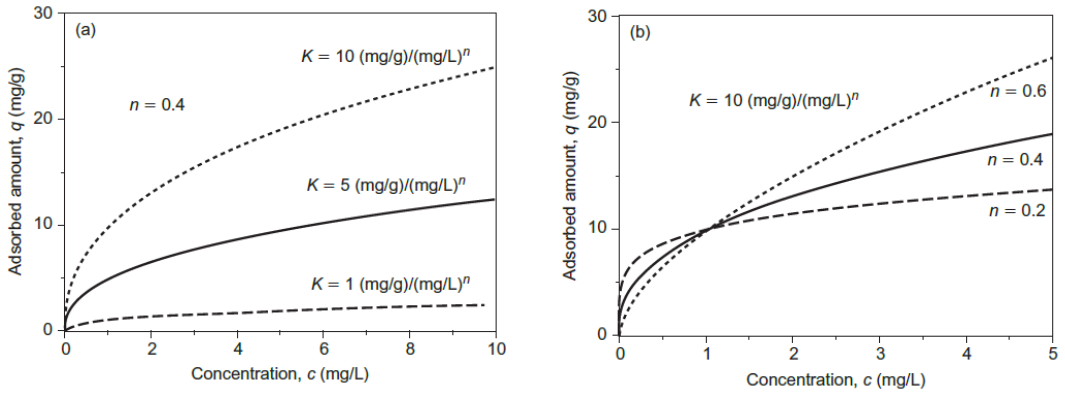

Figure 2.5: Influence of Freundlich isotherm parameters a) K, b) n on the shape of the isotherm (Worch, 2014).

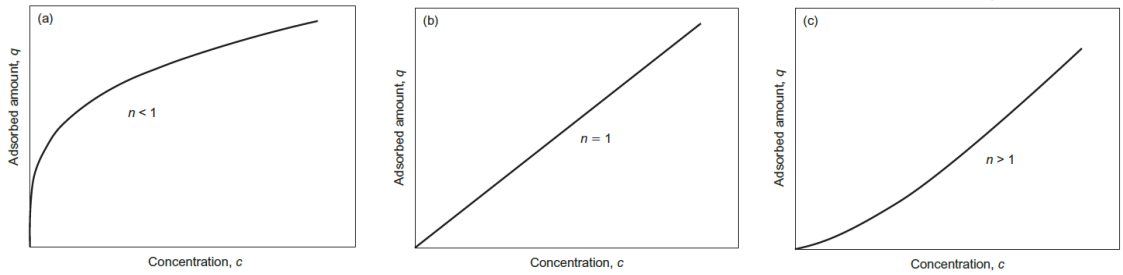

Figure 2.6: Different form of Freundlich isotherm: a) n<1, b) n=1, c) n>1 (Worch, 2014).

The Langmuir equation is used for small concentration ranges, assuming a homogeneous structure of the adsorbent surface, while the Freundlich isotherm is better to describe adsorption in aqueous solutions, describing data for heterogeneous solutions. Freundlich equation can be derived from the Langmuir equation, assuming a heterogeneous behavior of the adsorbent surface, which means a logarithmic decrease of the differential adsorption enthalpy with increasing solid-phase concentration (Sperlich, 2010).

Adsorption kinetics

In the adsorption process exists a time dependence, associated with the loading and the liquid-phase concentration. Adsorption kinetics explains this relationship, referred to the increase of the loading with time in one way, or the decrease of liquid-phase concentration in another way.

$$q_{eq} = f(t) \quad ; \quad c_{eq} = f(t) \tag{2.9}$$

To reach the state of equilibrium, which is not established instantaneously, a mass transfer process from the solution to the adsorption sites within the adsorbent particles is accomplished, which determines the time required to get to the balanced state.

At first the external mass transfer step of the adsorbate from the bulk solution to the hydrodynamic boundary layer around the adsorbent takes place, by liquid phase diffusion. Then the adsorbate diffuses to the inside of the porous adsorbent, defined as intraparticle diffusion, supposing pore or solid diffusion processes. Finally the adsorbate molecules and the final adsorption sites interact energetically. The rate of adsorption is controlled by the kinetics of bond formation (Worch, 2014).

2.4. Adsorption onto GFH

There is a number of material-dependent functional sites on the surface of the adsorbent. In the case of adsorbents based on metal (hydr)-oxides, these sites correspond to the external hydroxyl groups. The adsorption of cations could take place under this assumption. For example, by the substitution of the proton of a hydroxyl group for a cation (L. Sigg und W. Stumm, 1996).

Anions, on the other hand, are completely replaced by an OH group (ligand exchange). Furthermore, covalent or ionic bonds of the adsorptive (or adsorpt) to the adsorbent surface are also referred to as surface complexes. Figure 2.7 shows possible examples of such surface complexes and their names. In addition, the difference between the spherical and the inner spherical complexes, which differ from each other by different bond distances to the surface of the iron hydroxide, is illustrated (L. Sigg und W. Stumm, 1996).

An important factor for the description of adsorption processes on iron hydroxides is also the pH, since this has a direct influence on the surface charge of protein hydroxides. The affinity of adsorbent and adsorptive to each other is therefore positively or negatively

affected. A balanced surface charge is also called charge zero or pH_{pzc} (point of zero charge). Above the pH_{pzc}, the surface charge becomes negative and below correspondingly positive. Anionic adsorptives are thus attracted more strongly by the surface of an iron hydroxide at pH values below the pH_{pzc} (X.-H. Guan, 2007).

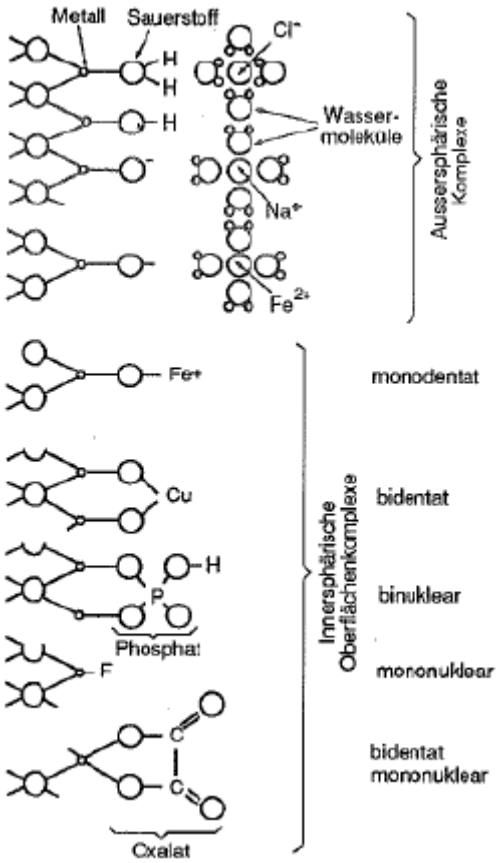

Figure 2.7: Different ions and types of binding to a metal hydroxide surface (L. Sigg und W. Stumm, 1996).

3. Material and methods

3.1. Adsorbent media

Granular ferric hydroxide (GFH)

Granular ferric hydroxide, developed between 1990 and 1994 by the department of Water Quality Control of Berlin Technical University and produced since 1997 by the company GFH Wasserchemie (Osnabrück, Germany), is a granular adsorbent used in fixed-bed water treatment systems.

GFH is a synthetically produced, weakly crystalline and porous adsorbent. 50-70 % of GFH consists of ironoxyhydroxide akaganèite (ß-FeO(OH)) and also Ferrihydrit ($Fe_5HO_8 \cdot 4H_2O$) and other iron(hydr)oxides. Akaganèite is meta-stable and differs from other iron(hydr)oxides as goethite (α-FeOOH) or hematite (α-Fe_2O_3) by its tunnel-like crystal structure. The pH_{PZC} is reported to be between 7.5 and 8.0 (Sperlich, 2010).

The particle size is lower than 0.3 mm and specific surface area reaches up to 300 m^2/g, larger than others like hematite or goethite. Table 3.1 below shows some important physicochemical properties of GFH.

Micro granular ferric hydroxide (µGFH)	
Composition	Synthetic Akaganèite (ß-FeO(OH)) and Ferrihydrit ($Fe_5HO_8 \cdot 4H_2O$) (Bahr, 2012)
Iron content	610 g/kg
Grain size	<0.3 mm
Porosity	aprox. 75 % (Bahr, 2012)
Specific surface area	300 m^2/g (Bahr, 2012)
Water content	aprox. 53 %

Table 3.1: Properties of micro-GFH

Provided GFH is consisted of the fine fraction of dried granular ferric hydroxide with a particle size lower than 0.3 mm. The material was sieved using a set of standard testing sieves (0.033-0.125 mm) to analyze the grain size distribution. The GFH for the experiments was taken directly from the provided recipient. To perform the experiments a 10 g/L GFH stock suspension was prepared.

Iron oxyhydroxide agglomerates

(Fe^{+3}) oxide/hydroxide nanoparticle-based agglomerate suspension, has been used as adsorbent for chromium and phosphate species. The material was prepared with a method provided by Technion, Israel Institut of Technology, resulting in nano-crystals with a high surface area. The process to prepare the agglomerates is next explained.

Ferric chloride is hydrolyzed in double distilled water at room temperature according to:

$FeCl_3 * 6H_2O \rightarrow NanoFe + HCl + H_2O$ (Zelmanov and Semiat, 2011)

280 gr of Ferric chloride were dissolved in 800 mL of double distilled water, obtaining a concentration of 350 g/L. The required concentration was 2 g/L, so 28.6 mL were extracted and dissolved in 5 L of DI water, calculated by,

$$C_1 * V_1 = C_2 * V_2 \quad (3.1)$$

known as “Dilution equation”, where C is the concentration, V is the volume and the indices represent the initial and final position respectively.

Then the solution was mixed for 24 hours and aged 120 hours in the dark. The mixture of iron oxides and hydroxides forms small crystals, with an acidic pH lower than 4 as a consequence, after this hydrolysis process.

The agglomerates were prepared by addition of NaOH until the desired pH was obtained, pH 6 in this case, using a dosing pump. The formation of iron oxyhydroxide agglomerates was finished after aging the solution for 120 h in the dark.

3.2. Batch experiments

Adsorption isotherms

Using GFH as adsorbent for phosphate, the isotherm was built by the variation of the initial concentration at constant adsorbent dose, following the general form of isotherm equation [2.4]. The initial concentration of phosphate was 4 mg/L for every experiment. The desired GFH concentration was calculated by the liquid-to-mass ratio, which is listed in Table 3.2, depending on the pH value.

For chromium adsorption, the experiments were performed at a constant adsorbent concentration dose (0.5 g/L), varying the adsorbate initial concentration dose from 0.25 to 4 mg/L following Asgari *et al.*, (2008). The conditions were the same for every analyzed case. Isotherms were calculated following equation [2.4].

The isotherms were developed in different water matrixes, to study the effect of the composition in the adsorption process. De-ionized water (DI), Berlin drinking water (DW), and DI water with a concentration of 10 mmol NaCl per liter were used. Every sample consisted of 200 mL solution, the volume of water was calculated by the difference between the entire volume and the already set volumes of adsorbent and adsorbate, everything in 250 mL crystal bottles.

Constant pH-conditions were reached by adding 2 mmol/L of one of the biological buffer substances MES (2-(N-morpholino)ethanesulfonic acid, pKA = 6.1), BES (N,N-Bis(2-hydroxyethyl)-2-aminoethanesulfonic acid, pKA=7.1) and TAPS (N-Tris(hydroxymethyl)methyl-3-aminopropanesulfonic acid, pKA=8.4). After preparation of the model water matrix, pH was adjusted to 6, 7 and 8, respectively, using HCl or NaOH (Sperlich, 2010)**.**

With the agglomerate as adsorbent, the isotherms were developed with a fixed adsorbent concentration of 2 g/L and changing the adsorbate dose, from 2 up to 50 mg/L for chromium and from 1 up to 12 mg/L for phosphate, in 200 mL solution, following [2.4].

To obtain the different points of the isotherms it was decided in this case to variate the initial concentration of adsorbate and change the adsorbent dose. To complete the 200 mL solution, de-ionized (DI) water was used as matrix, in 250 mL crystal bottles. The isotherms were developed at pH 6, the one with highest efficiency, already reached in the preparation of the agglomerate (Technion, 2017).

All the experiments were performed at room temperature (20±1°C). The samples were shaken for 96 hours for phosphate and 24 h for chromate. This is the time needed to reach the equilibrium. The adsorbate was added right before the start of mixing time, as

the last step of the preparation. The samples began the shaking time one by one every 5 minutes, so it was possible to control the exact contact time. The adsorbent was removed via vacuum filtration with a 0.45 µm cellulose nitrate filter. Final concentrations were analyzed by the methods FIA, AAS and IC, next explained.

KH_2PO_4 (m=136.09 g/mol) was used to prepare a 50 mg/L P solution, which was filtrated and kept for 15-20 min in ultrasonic water. Chromium solution was prepared with $Na_2Cr_2O_7*2H_2O$ (m=298 g/mol), with a concentration of 1 g/L.

All conducted experiments are listed below in table 3.2.

Water matrix	***Adsorbent***	***pH***	***L/m [L/g]***	***Adsorbent[g/L]***	***Adsorbate[mg/L]***	***Data source***
DI	GFH	8±0.2	3.2-12.8	0-0.39	4 [P]	(Sperlich, 2010)
DI + NaCl	GFH	8±0.2	3.2-12.8	0-0.5	4 [P]	
DI + NaCl	GFH	7±0.2	3.2-25.7	0-0.46	4 [P]	
DI + NaCl	GFH	6±0.2	3.1-23.7	0-0.48	4 [P]	
DW	GFH	7±0.2	3.2-25.7	0-0.46	4 [P]	
DI	GFH	8±0.2	2	0.5	0.25-4 [Cr]	(Asgari *et al.*, 2008)
DI	GFH	7±0.2	2	0.5	0.25-4 [Cr]	
DI	GFH	6±0.2	2	0.5	0.25-4 [Cr]	
DI + NaCl	GFH	7±0.2	2	0.5	0.25-4 [Cr]	
DW	GFH	7±0.2	2	0.5	0.25-4 [Cr]	
DI	AGG	6±0.2	0.5	2	1-12 [P]	-
DI	AGG	6±0.2	0.5	2	2-50 [Cr]	(Lazaridis, 2004)

Table 3.2: Batch isotherm experiments

Flow injection analysis (FIA)

Equilibrium concentrations of phosphate were analyzed by flow injection analysis using FIAstar® 5000.

Flow injection analysis (FIA) is based on the injection of a liquid sample into a moving, nonsegmented continuous carrier stream of a suitable liquid. The injected sample forms a zone, which is then transported toward a detector that continuously records the changes in absorbance, electrode potential, or other physical parameter resulting from the passage of the sample material through the flow cell (Kikas, 2014).

Atomic adsorption spectrometry (AAS)

Atomic adsorption spectrometry (AAS) is an analytical technique that measures the concentrations of elements. The technique makes use of the wavelengths of light specifically absorbed by an element. They correspond to the energies needed to promote electrons from one energy level to another, higher, energy level (Dale, 1982).

Equilibrium concentration of chromate adsorption onto agglomerates was measured by the PerkinElmer PinAAcle 900 spectrometer. The PerkinElmer PinAAcle 900 spectrometer system is a compact high-atomic absorption spectrometer with built - in burner system flame atomization and graphite tube furnance for electrothermal atomization. The spectrometer can perform fully one-cell analyzes from a connected computer using the software Winlab32 for AAS controlled (Back, 2012).

Ionic chromatography (IC)

Adsorption chromatography depends upon interactions of different types between solute molecules and ligands immobilized on a chromatography matrix. The first type of interaction to be successfully employed for the separation of macromolecules was that between charged solute molecules and oppositely charged moieties covalently linked to a chromatography matrix. The technique of ion exchange chromatography is based on this interaction (Biotech, 1991).

Equilibrum concentration of chromate adsorption onto GFH was measured by the Methro compact IC flex.

4. Results and discussions

4.1. Physical characterization of GFH

Figure 1 shows the grain size distribution of micro GFH particles, sieved with 0.033, 0.063, 0.09 and 0.125 mm and classified in the ranges 2-63, 63-120 and > 120 µm. It is possible to observe in the figure below that the particles with a size higher than 120 µm have an important mass contribution to the total volume, with a fraction of 43.7%, almost half of the global quantity. It is important to remark that the higher mass consists of only a few particles with bigger grain size.

The rest of analyzed fractions are equally large. Particles in the range from 2 to 63 µm have a fraction of 26.7%, while the contribution for the 63-120 µm range is higher, having a percentage of 29.65.

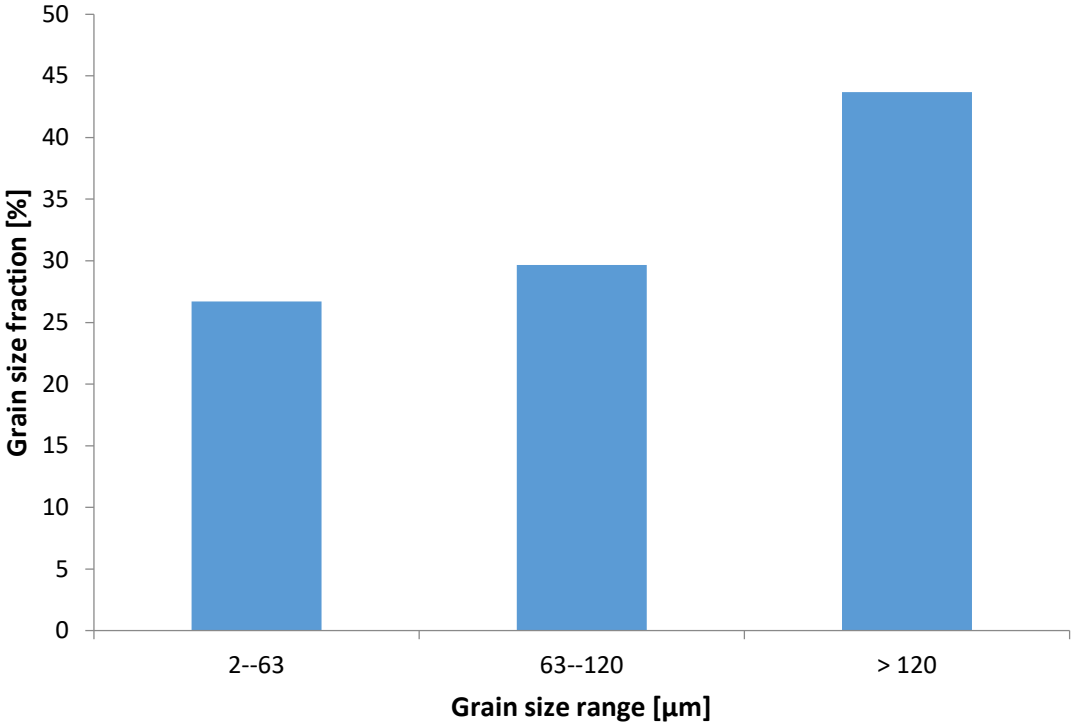

4.2. Iron oxyhydroxide agglomerates characterization

A visual study was made to observe the effect of ranging pH from 3-12 on the formation of the agglomerate. 200 mL of DI water with agglomerate solution were prepared and placed into 250 mL glass bottles. The pH was modified by the addition of NaOH or HCl. The analysis was then compared to the information provided by Technion University.

Due to the pH curve, obtaining the exact pH increments proved to provide a challenge. Extra attention was required when preparing the pH increments between pH 6-9. It was not possible to effectively prepare the solution with a pH of 9. As such, it has been excluded from the analysis.

In Technion University´s results, it is possible to see a homogeneous solution without a deposition layer in bottles pH 3 and pH 4. A progressive reduction of the deposition layer in bottles pH 5-12 (excluding 9) was observed. This is in contrast to the AdsFiltTUB experiment, where the progression reduction is not seen. However, colors of each corresponding deposit layers, between the two experiments are similar.

The formation of agglomerates starts to form at pH 4. The agglomerate with a clear deposition layer is seen at pH 5, but the formation of a deposition layer begins to be noticable at pH 4. The complete agglomeration as isolated grains is observed at pH > 6.

It was observed, that the more alkaline the pH is, the more compact the agglomerate, the smaller the grain size and the more intense the brown-red color of the deposition layer becomes.

It is possible to see all the commented results in the following pictures.

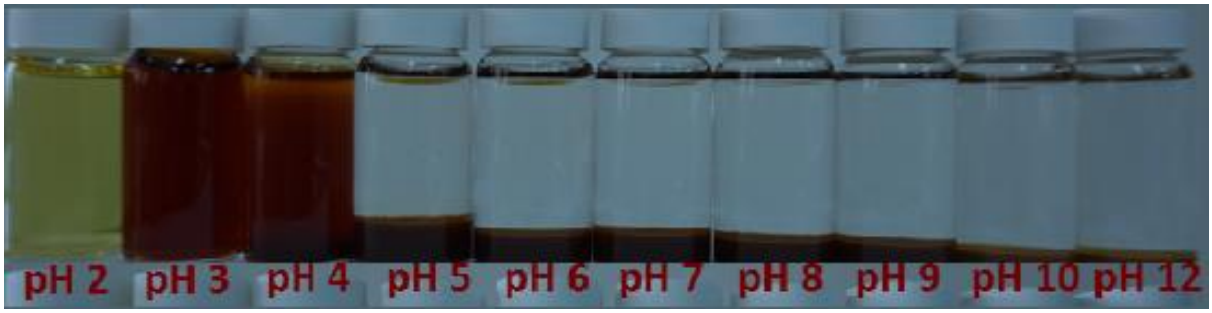

Figure 4.1: Effect of pH on agglomerate (Technion, 2017).

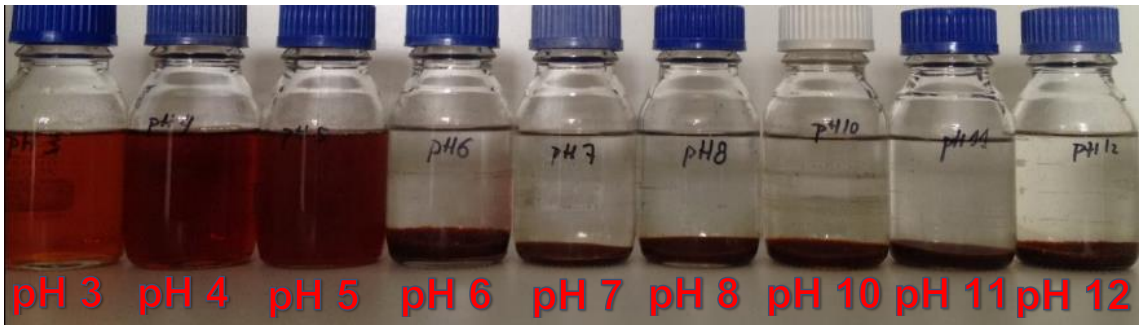

Figure 4.2: Effect of pH on agglomerate

.

4.3. Batch adsorption experiments

Phosphate adsorption isotherms

The objective was to compare the effects of pH and water matrix on the adsorption equilibrium of phosphate. For the study, the parameters were selected following the criteria listed in Sperlich [2010]. The final results were also compared to this source. All the experiments were performed by changing the concentration of GFH in the liquid-to-mass ratio. Each experiment had a starting concentration of 4 mg/L P. Freundlich isotherms were linearized by transforming the equation [2.6] into the logarithmic form [2.7]. Using the Freundlich parameters, the isotherms were drawn in each case.

The adsorption of phosphate onto GFH is believed to be dominated by complexation between surface groups and the adsorbing molecules. Depending on pH, the GFH surface sites react as acid or base, resulting in a pH-dependent surface charge causing electrostatic interactions with the surrounding aqueous phase (Sperlich, 2010).

Figure 4.3 shows the phosphate adsorption isotherms with the effect of different pH, using DI as the water matrix, with 10 mmol/L of NaCl. The first conclusion drawn, is that the lower the pH, the more efficient the adsorption. The adsorption efficiency is clearly affected by the pH value. As the pH increased, there is a significant decrease in adsorption.

Below its pH_{PZC} of 7.5 - 8.0, GFH is a positively-charged adsorbent. Phosphate is an anionic adsorbate in monovalent ($H_2PO^-_4$) and divalent (HPO^{2-}_4) form. Above pH 7.1, the more negative, divalent HPO^{2-}_4 will be the dominating phosphate species in solution. Also, the surface charge of GFH becomes more negative with increasing pH, resulting in more neutral and negatively charged groups on the surface. This explains the sharper decrease

in adsorption capacity from pH 7 to 8 compared to the less pronounced decrease from pH 6 to 7 (Sperlich, 2010).

The results were compared with data from Sperlich [2010] and observed to be similar. Starting with pH 6, the capacity values are almost matching and the Freundlich isotherm has the same logarithmic trend-line.

For pH 7, the values do not look that exact, but the logarithmic trend-line of Freundlich is very similar up to the equilibrium concentration of 2 mg/L P of the Sperlich [2010] results. PH 7 is close to the pH_{PZC} (between 7.5 and 8), where the surface of GFH changes their charge from positive to negative. The pH value was measured with an error of ± 0.2. The capacity values are higher for Sperlich [2010] at pH 7. A difference of the pH values (inside the interval $\pm$ 0.2) could charge the GFH surface differently. It is very close to the point of zero charge, so the difference of achieved adsorbent loadings could be perceptible. The surface charge of GFH can be affected by small changes of the pH value close to the point of zero charge.

The isotherms with pH 8 show almost the exact same capacity values, such that the trend line mimics the Sperlich [2010] results.

In summary, the obtained results were well approximated to Sperlich [2010]. The capacity values were similar for all cases, such that the Freundlich isotherms are the same. This means that µGFH performs similar to GFH with bigger particles sizes for the adsorption of phosphate.

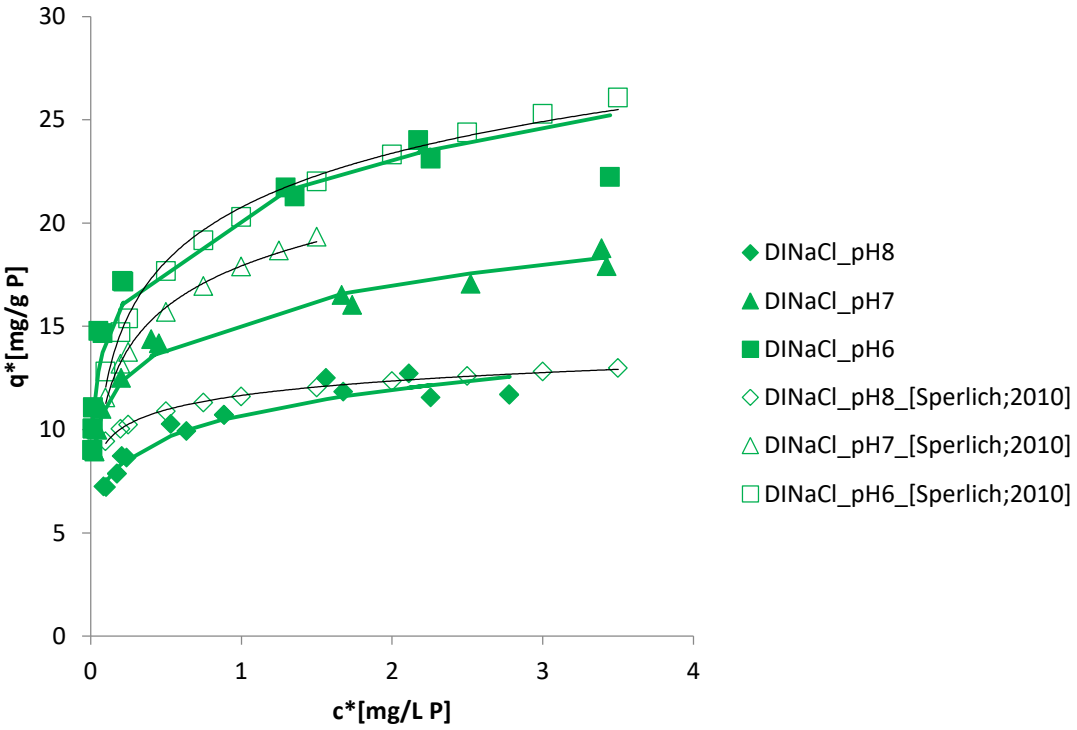

Figure 4.3: Batch adsorption isotherms of phosphate onto GFH at different pH values in DI water with 10 mmol/L NaCl; c0=4 mg/L P, cGFH= ca. 0-500 mg/L and comparison with isotherms from Sperlich [2010]

In figure 4.4 the adsorption batch isotherms for different water matrixes performed at pH 7 are shown, with the objective to analyze the influence of the water matrix on the adsorption equilibrium. Two matrixes were analyzed, Berlin drinking water (DW) and DI water with NaCl content of 10 mmol/L.

Berlin drinking water (DW) shows higher capacity values than DI water, which means that the adsorption was more efficient for DW, with a higher achieved adsorbed concentration. Comparing maximum adsorbed capacity values listed in table 4.1, the difference is not very significant, with 18.78 mg/g P for DI water and 25 for DW.

"Adsorption of positively charged calcium ions onto the GFH surface shifts the pH_{PZC} to higher values, thus improves the adsorption of phosphate. Also, calcium might facilitate double-layer adsorption of phosphate" (Sperlich, 2010).

Results were compared with Sperlich [2010]. For DW, capacity values and logarithmic trend-lines of Freundlich are very similar up to the equilibrium concentration of 1 mg/L P. The case of DI water at pH 7 is analyzed in Figure 4.3.

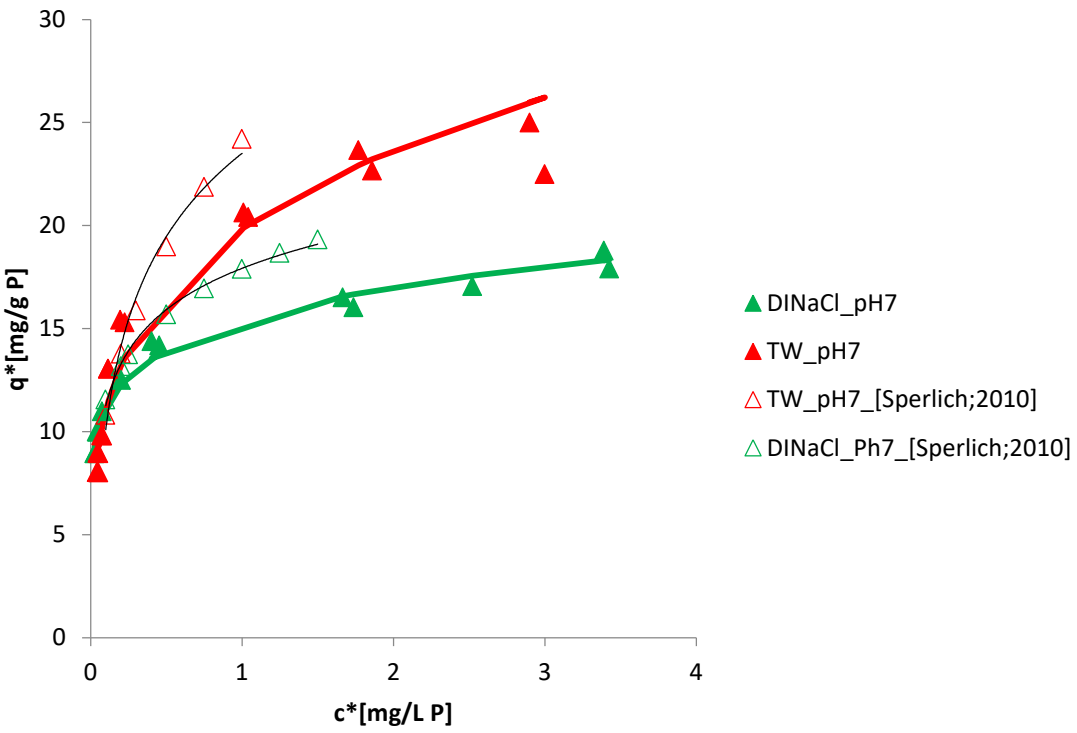

Figure 4.4: Batch adsorption isotherms of phosphate onto GFH with different water matrixes at pH 7. c0=4 mg/L P; cGFH=0-480 mg/L for DI water with 10 mmol/L NaCl and DW, and comparison with Sperlich [2010].

Figure 4.5 shows the influence of NaCl on the batch adsorption isotherms at pH 8.

The achieved adsorbent loading is higher for DI water with NaCl, thus a stronger adsorption. However the values are very similar for both cases. It does not exist a notable difference between maximum capacity values, 12.71 mg/g P for DI water with NaCl and 13 mg/g P (Table 4.1).

Freundlich isotherms for both matrixes describe the same logarithmic trend-line and are almost matching. The isotherm from Sperlich [2010] of DI water with NaCl content was also drawn in the graph. As it is observed, the results are almost equal. The maximum value of capacity is 13 mg/g P, which means a non-significant difference compared to the maximum capacity value of 12.71 mg/g P.

In summary, the effect of NaCl addition can help to achieve a higher adsorbent loading although the difference is not significant, but it can improve the adsorption efficiency of phosphate onto GFH slightly.

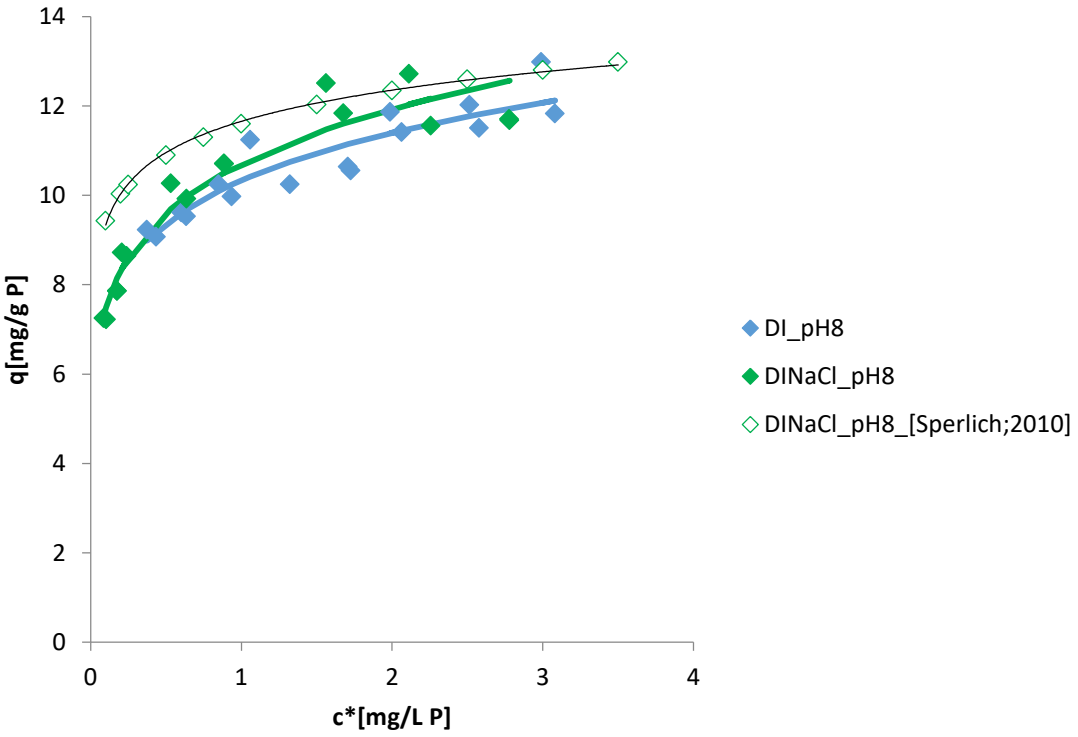

Figure 4.5: Batch isotherms of phosphate onto GFH with different water matrixes (DI and DI with 10 mmol/L NaCl) at pH 8; c0=4 mg/L P; cGFH=0-500 mg/L and comparison with Sperlich [2010].

Results were evaluated using Freundlich (2.6) and Langmuir (2.5) isotherm equations, frequently used for the characterization of isotherm data.

Freundlich and Langmuir constants are summarized in Table 4.1. To contrast the results, as a second analysis of the study, the Freundlich and Langmuir constants from Sperlich [2010] are also listed in Table 4.1.

Freundlich "n" coefficients are lower than 1 for every case, all in a range from 0.1 to 0.4. The values are very similar comparing to the "n" constants of Sperlich [2010]. Regression coefficients "R^2" are all in an interval from 0.8 to 1, which shows a good linearity of the data.

Comparing to Sperlich [2010], K_F constants are very similar for the adsorption in DI water with NaCl content at different pH values, so are the Langmuir maximum adsorbent concentration, q_m, constants.

The highest value of K_F (20.65) is at pH 6, associated to a q_m, of 24.01 mg/g P. The minimum value of K_F (10.7) is associated to the minimum q_m value (12.71) at pH 8.

The achieved loading in DW is higher than in DI with NaCl content for the same pH value. Table 3.1 shows that constant K_F in DW (19.83) is therefore higher than K_F in DI with NaCl content (15.41) at pH 7 with maximum adsorbed concentrations, q_m, of 25 and 18.78 mg/g P respectively. It is also shown that the constant values from Sperlich [2010] are very similar for both constants.

The adsorption strength at pH 7 (K_F=10.32) was much lower than the most efficient cases such as the adsorption in DW at pH 7(K_F=19.83; q_m=25 mg/g P) or adsorption in DI with NaCl content at pH 6 (K_F=20.65; q_m=24.01 mg/g P), concluding that pH 6 and DW as water matrix present the highest adsorption potential, phosphate adsorption onto GFH is pH and water matrix dependent.

MATRIX	**ADSORBENT**	**pH**	**FREUNDLICH**			**LANGMUIR**	**SOURCE**
			K_f	**n**	**R^2**	**q_m**	
			*	**[-]**		**[mg/g]**	
DI+NaCl	GFH	6.2±0. 2	20.3	0.2	0.91	23.9	(Sperlich, 2010)
DI+NaCl	GFH	7.1±0.2	17.9	0.19	0.93	18.4	(Sperlich, 2010)
DI+NaCl	GFH	8.1±0.2	11.6	0.09	0.81	13	(Sperlich, 2010)
DW	GFH	7±0.2	24.2	0.35	0.98	26.7	(Sperlich, 2010)
DI+NaCl	GFH	6±0.2	20.65	0.16	0.95	24.01	AdsFiltTUB
DI+NaCl	GFH	7±0.2	15.41	0.14	0.98	18.78	
DI+NaCl	GFH	8±0.2	10.7	0.15	0.94	12.71	
DW	GFH	7±0.2	19.83	0.25	0.94	25	
DI	GFH	8±0.2	10.32	0.14	0.85	13	

* $[L^n/(g*mg^{n-1})]$

Table 4.1: Isotherm model parameter: Freundlich and Langmuir coefficients.

Chromate adsorption isotherms

The second part of the study was to analyze the influence of pH and water matrix on the chromium adsorption equilibrium.

Liquid-to-mass ratio was modified by changing initial concentrations of chromium from 0.25 to 4 mg/L and having a fixed GFH concentration of 0.5 g/L (Asgari *et al.*, 2008). Experiments were performed at pH 6 to 8 in DI, DW and DI with 10 mmol/L NaCl content.

Freundlich isotherms were linearized by transforming the equation [2.6] into the logarithmic form [2.7]. Using the Freundlich parameters, the isotherms were drawn in each case.

Figure 4.6 shows batch adsorption isotherms in DI water at different pH values up to equilibrium concentration of 0.5 mg/L Cr. The most efficient adsorption was at pH 6, with higher capacity values than at pH 7 and 8. The highest achieved capacity was q_m= 7.56 mg/g Cr, with a significant difference to the maximum capacity at pH 8 (q_m=2.97 mg/g Cr). The obtained capacity of the adsorption at pH 7 presents a value in between, with q_m= 5.11 mg/g Cr. Thus chromium adsorption is pH dependent. Adsorption potential is higher for lower pH.

Freundlich isotherms describe a logarithmic trend-line and present a concave shape with respect to the concentration axis, Freundlich “n” coefficients are for every case lower than 1.

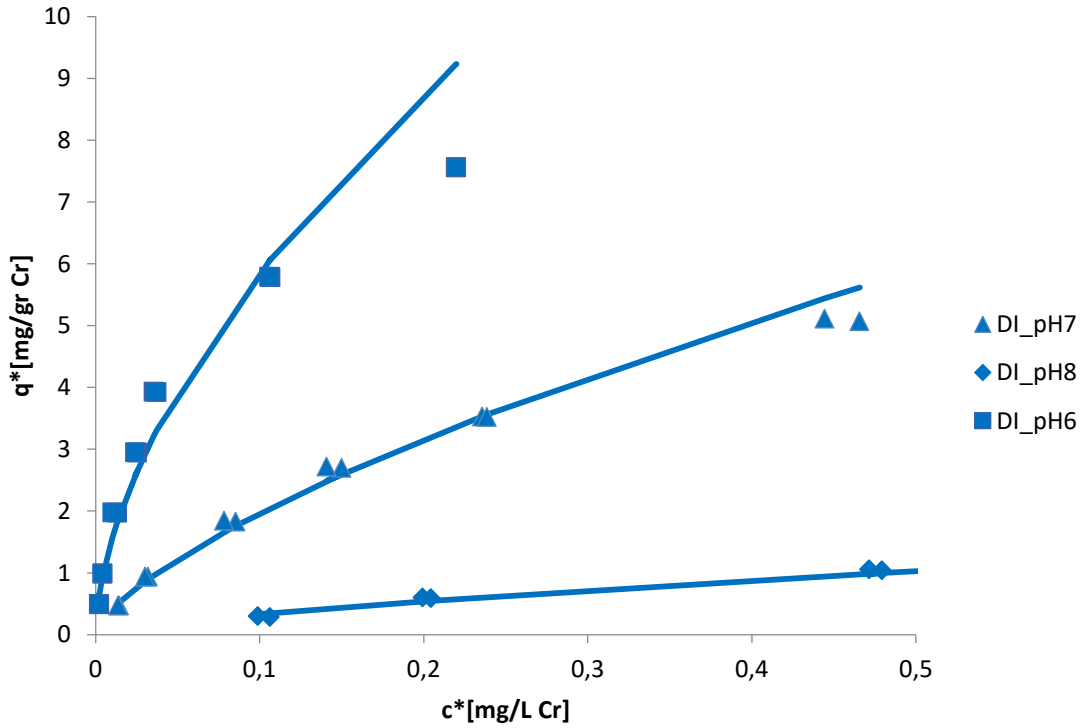

Figure 4.6: Batch adsorption isotherms of chromium onto GFH at pH 6, 7, 8 in DI water; c0= 0.25-4 mg/L Cr; cGFH=0.5 g/L.

In Figure 4.7 chromate batch adsorption onto GFH isotherms at pH 7 in different water matrixes (DI, DI with 10 mmol/L NaCl and DW) are shown, up to equilibrium concentration of 0.8 mg/L Cr.

Isotherms performed in DI water are almost matching, describing the same logarithmic trend-line. The capacity values are very similar, which means that the effect of NaCl is not significant. The highest achieved loadings are approximatly, 5.1 mg/g Cr for DI water and 6.2 mg/g Cr for DI water with NaCl content.

Batch adsorption isotherm in DW shows much lower capacity values compared to isotherms in DI water. The maximum capacity value in DW is 2.97 mg/g Cr.

Berlin DW contains components which could affect the adsorption process. Particularly, sulfate ions compete with chromium in the process, interacting as well with GFH. The presence of other competing anions like chloride or silicate could also affect the adsorption process. The interfering effect could be a reason for a less efficient chromium adsorption, achieving lower adsorbent loadings. This is possible to observe in Figure 4.7.

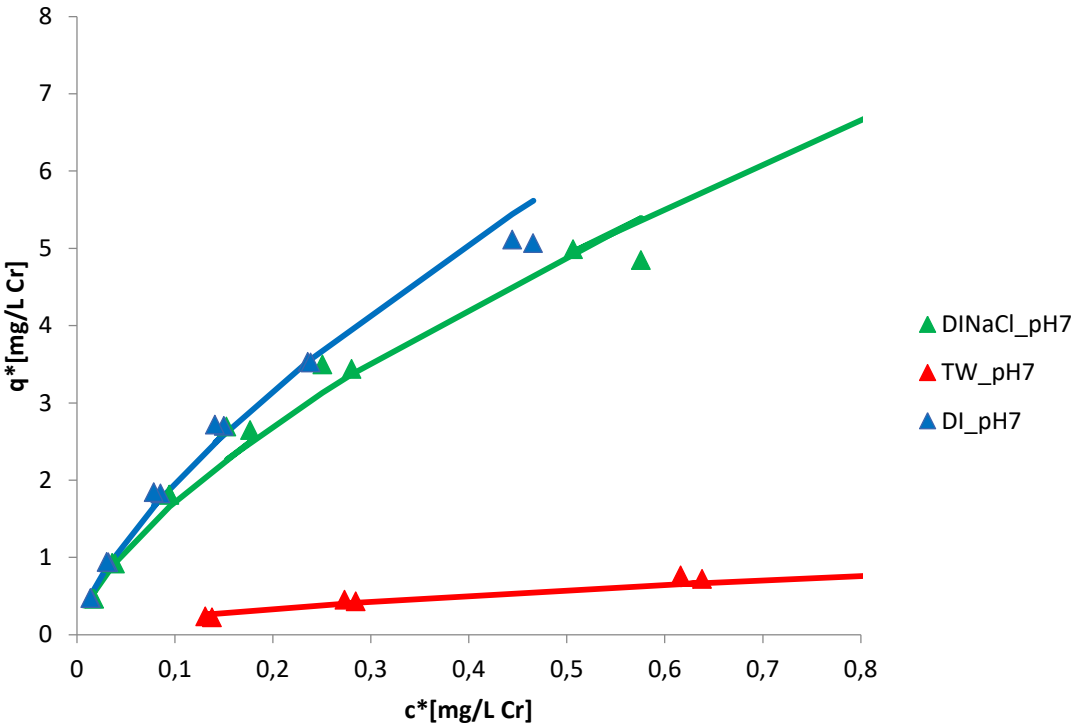

Figure 4.7: Batch adsorption isotherm for GFH in different water matrixes(DI, DI with 10 mmol/L and DW water) at pH 7; c0= 0.25-4 mg/L Cr; cGFH= 0.5 g/L.

In Table 4.2 isotherm constants of Langmuir and Freundlich are shown. Freundlich coefficient "n" is for every case lower than 1, in an interval from 0.6 to 0.7, which means a concave shape of the isotherms. The Freundlich regression coefficients, "R^2" have values very close to 1, from 0.96 to 0.98, which signifies that the two variables being compared have a perfect positive relationship. The closer the value of R^2 is to 1, the stronger the linear relationship

Analyzing isotherm parameters in DI water at different pH values, the highest value of K_F (22.16) is at pH 6, associated to a q_m, of 7.56 mg/g P. The minimum value of K_F (1.67) is associated to the minimum q_m value (2.97) at pH 8.

Remarkably the lowest capacity of all, occurs in DW as matrix, with a value of 1.65 mg/g Cr associated also to the lowest K_F constant, 0.87. In contrast to phosphate adsorption, adsorption in DW does not present an efficient adsorption.

Comparing adsorption in DI and DI with 10 mmol/L NaCl content, maximum achieved loadings q_m present similar values but the value of K_F for the second case is 7.73, which is not very high according to the value of q_m, 6.29 mg/g Cr, while in DI water the value of K_F is the highest of all examined cases, 22.16, associated to the highest capacity of all, 7.56

mg/g Cr.

Chromium adsorption onto GFH is pH and water matrix dependent. Isotherms performed at lower pH (in the range from pH 6 to 8) can achieve higher adsorbent loadings. The presence of NaCl in DI water does not have a significant effect on the adsorption and adsorption in DW water is less efficient.

MATRIX	**ADSORBENT**	**pH**	**FREUNDLICH**			**LANGMUIR**
			K_F	**n**	**R^2**	**q_m**
			*****	**[-]**		**[mg/g]**
DI	GFH	6±0.2	22.16	0.57	0.96	7.56
DI	GFH	7±0.2	9.45	0.68	0.99	5.11
DI	GFH	8±0.2	1.67	0.7	0.98	2.97
DI+NaCl	GFH	7±0.2	7.73	0.65	0.98	6.29
DW	GFH	7±0.2	0.87	0.59	0.97	1.65

***** $[L^n/(g*mg^{n-1})]$

Table 4.2: Isotherm model parameter. Freundlich and Langmuir coefficients.

Adsorption with agglomerates

A second part of the study was to analyze the influence of pH and water matrix on adsorption equilibrium of chromium and phosphate onto the nano-particles based agglomerates suspension.

For the study, the parameters were selected following Technion (2017) and Lazaridis (2004) criteria.

“The adsorption is more efficient in the pH range from 5.5 to 6.5, which favors the attraction of metal ions and assures the stability of the sorbent material” (Lazaridis, 2004). The experiments were performed at pH 6 in DI water.

Experiments where performed without the presence of NaCl, as salinity suppresses chromium adsorption. The higher the concentration of NaCl, the less efficient the chromium adsorption (Technion, 2017). This effect occurs with NaCl concentrations higher than 1 mol/L.

The liquid-to-mass ratio was modified by having an adsorbent concentration of 2 g/L and varying the adsorbate concentration from 1 mg/L up to 12 mg/L for phosphate and from 2 up to 50 mg/L for chromium.

Figure 4.8 shows the batch adsorption isotherm of chromium onto agglomerates. The isotherm from Technion (2017) is also drawn. The conditions are the same, 2 g/L of adsorbent and pH 6. The experiments were performed with a concentration of chromium up to 50 mg/L which is not realistic in the industrial water treatment. The isotherms are developed up to equilibrium concentration of 10 mg/L Cr.

The maximum adsorbent loading achieved is much higher for Technion (2017), with a notable difference between the isotherms. The maximum capacity value is 6.4 mg/g Cr, while in Technion (2017) is 27 mg/g Cr. The Freundlich isotherms do not have similar trend-lines because of the significant difference of capacity values.

The experimental isotherm does not present an efficient adsorption. However the chromium adsorption onto agglomerates at pH 6 can achieve high adsorbent loadings, as was shown in Technion (2017) results. The inexperience with the production of the agglomerates could be a reason of the low adsorbent loadings achieved.

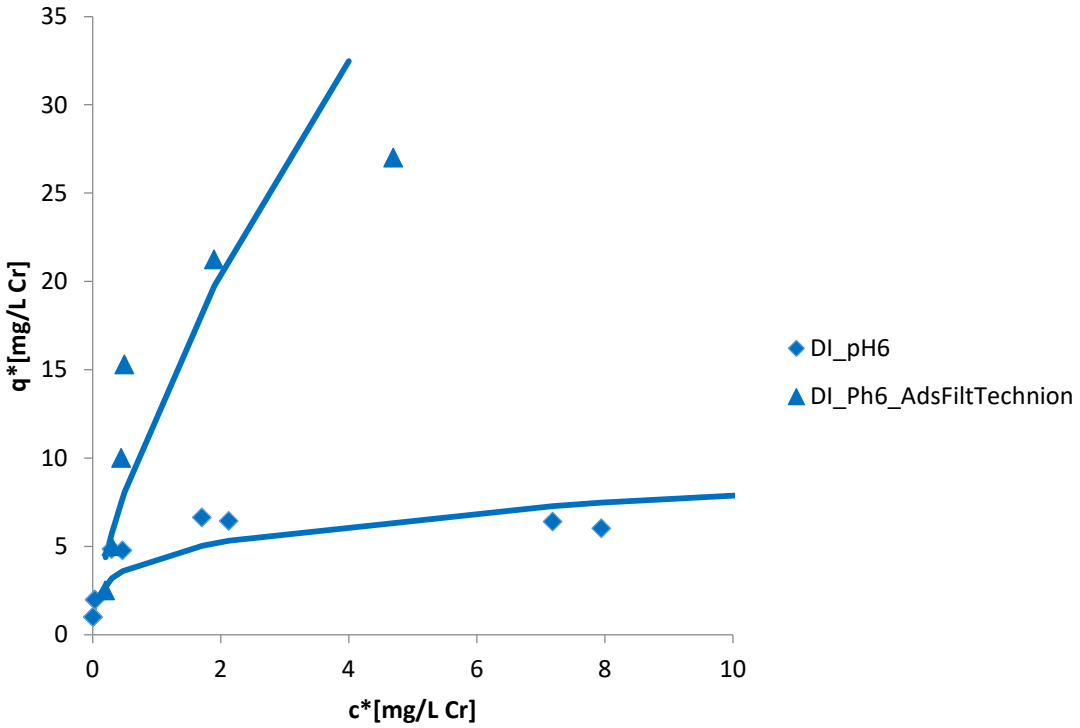

Figure 4.8: Batch adsorption isotherm of chromium onto agglomerates in DI water at pH 6; c0= 1-50 mg/L Cr; cAGG= 2 g/L.

Figure 4.9 shows the chromium batch adsorption isotherm onto agglomerates in contrast to GFH isotherm at pH 6 in DI water. The dose was 0.5 g/L for GFH and 2 g/L for the agglomerate. The isotherms were compared up to an equilibrium concentration of 0.5 mg/L.

The adsorbent dosage was higher for the agglomerate, however GFH presents a more efficient adsorption, achieving higher adsorbent loadings at the same pH and for DI as water matrix.

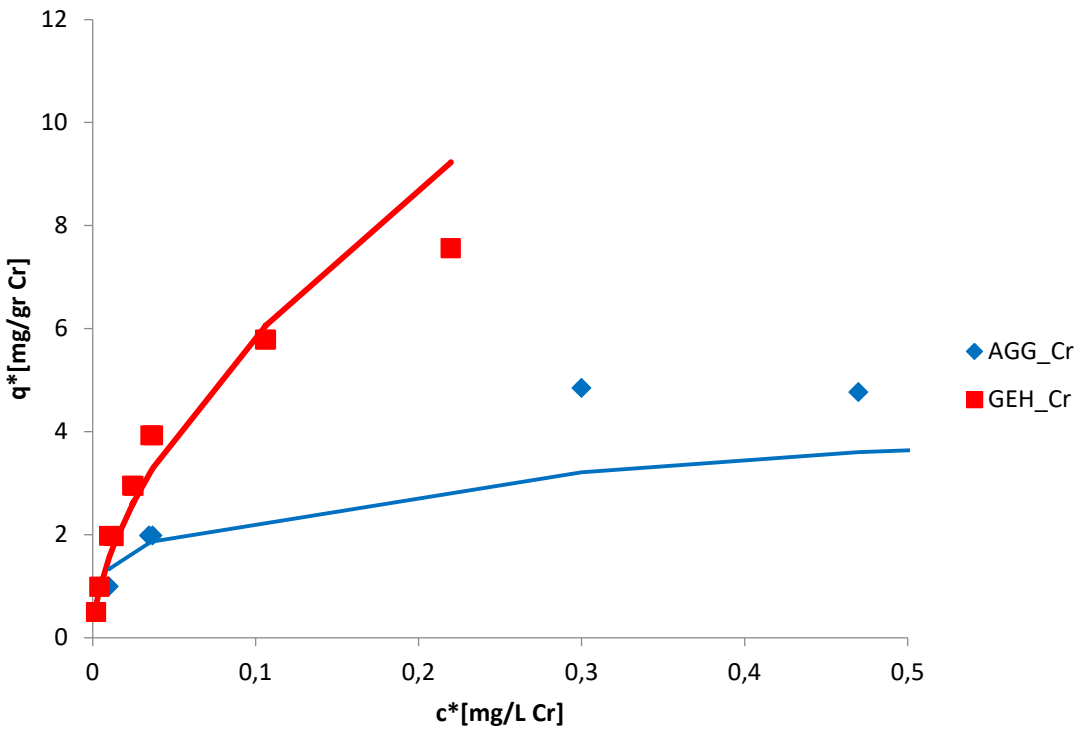

Figure 4.9: Comparison of batch adsorption isotherms for chromium onto different adsorbents, GFH (c0=0.25-4 mg/L Cr; cGFH=0.5 g/L) and agglomerates (c0=1-50 mg/L Cr; cAGG=2 g/L) in DI water at pH 6.

The last studied case is the comparison of phosphate adsorption onto agglomerates and GFH, shown in Figure 4.10. Adsorbent dosage varied from 0 to 0.48 mg/L GFH and 2 g/L for agglomerates.

The difference of capacity values is significant, much higher for phosphate adsorption onto GFH, reaching a maximum capacity of 24 mg/g P, while for the agglomerates the maximum achieved loading was 3.2 mg/g P.

In summary, using GFH as adsorbent offered a stronger adsorption potential for the analyzed cases with lower dosage concentration than the agglomerates.

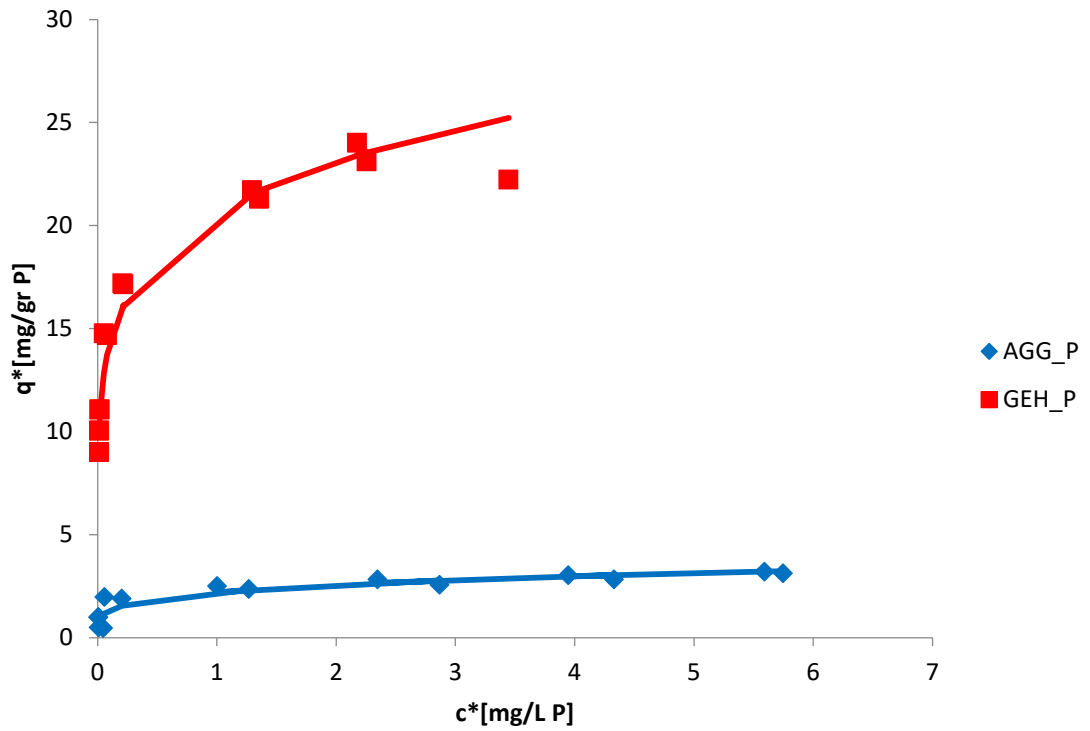

Figure 4.10: Comparison of batch adsorption isotherms for chromium onto different adsorbents, GFH (c0=4 mg/L Cr; cGFH=0-0.48 g/L; DI water with 10 mmol/L NaCl) and agglomerates (c0=1-12 mg/L Cr; cAGG=2 g/L; DI water) at pH 6.

Possible sources of errors

The variable GFH concentrations used were not inside the liquid-to-mass ratio interval of values listed in Table 3.2 for every phosphate adsorption case. The isotherms developed with concentration dosages only from inside the concentration intervals shown in Table 3.2 were incomplete, so it was necessary to use concentration values also from outside the intervals to achieve right isotherms.

According to Sperlich [2010], every pH case was associated with a different GFH concentration interval (Table 3.2). The pH was controlled in every step of the experiment, although some GFH concentration values were outside the interval defined by every pH.

Figure 4.11 a) shows an incomplete isotherm developed with dosage concentrations from inside the interval, in DI water at pH 8. Table 3.2 shows that the GFH concentration interval is 0-0.39 g/L. It was not possible to achieve low phosphate equilibrium concentrations, so the isotherm was not complete. For the rest of phosphate adsorption experiments, intervals were modified to achieve complete isotherms.

Figure 4.11 b) shows an unsuccessful isotherm with random values. This case was chromium adsorption onto GFH. The first experiments were performed with unrealistically high chromium concentrations of 50 mg/L. The results did not show in any case an isotherm describing a proper adsorption behavior.

An important fact to remark is the way of using the pipette for the adsorbent GFH stock suspension. The particles deposit at the bottom of the bottle, so it is important that the suspension is mixed by the time the GFH is extracted. The suspension must be homogeneous to extract the required concentration. Every extraction should be taken in the same point of the GFH suspension, at the same distance to the hole created by the revolution of the suspension when being stirred, to assure that the concentration is right. The extraction from the bottle should be slowly, lifting up the push bottom from the pipette carefully at constant speed. Once it is extracted, insert the GFH from the pipette to the required solution. The push bottom should be pressed at constant speed.

Figure 4.11 c) shows an example of the inconclusive experiments, with random values in the results and a non-logarithmic trend line, due to the inappropriate extraction of GFH adsorbent concentration.

a)

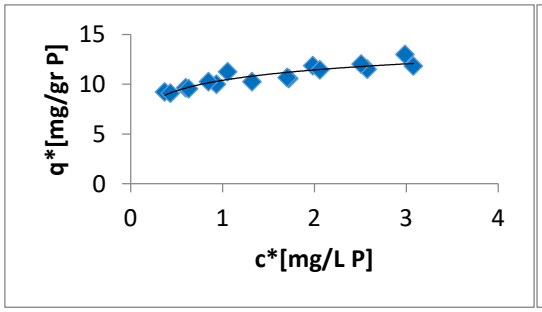

b)

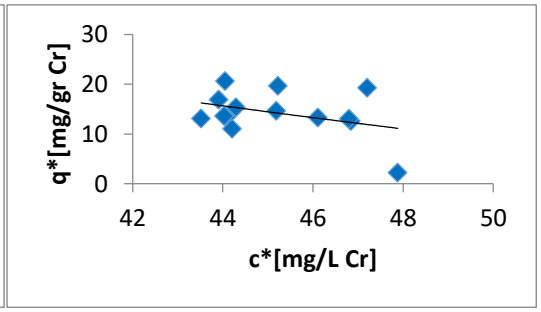

c)

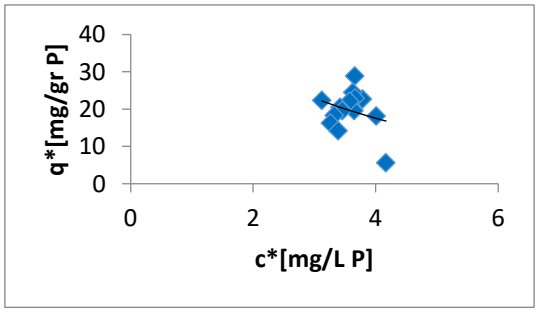

Figure 4.11: Unsuccessful batch adsorption isotherms: a) Isotherm not completed, phosphate adsorption onto GFH in DI water at pH 8. Lowest adsorbent loadings were not achieved; c0=4 mg/L; cGFH=0-0.39 g/L. b) Adsorption of chromium onto GFH. Experiment performed with high chromium concentrations; c0=50 mg/L Cr c) Unsuccessful isotherm due to inappropriate GFH extraction. Phosphate adsorption onto GFH in DI water at pH 8.

5. Conclusions and outlook

- Physical characterization of µGFH shows that a few number of particles with biggest size (> 120 µm) have the highest mass contribution.

- Phosphate adsorption is pH dependent. Maximum capacity reached at pH 6 was 24 mg/g P for an equilibrium concentration of 2mg/L. Maximum capacity reached at pH 8 was 13 mg/g P for the same equilibrium concentration

- Phosphate adsorption is water matrix dependent. Berlin DW shows the most efficient adsorption, which could be attributed to the presence of calcium. DI water shows a little improvement in the adsorption with a content of NaCl.

- GFH is suitable to remove phosphate from waste water. Highest adsorbent loadings are achieved with DW as water matrix and pH 6.

- Chromate adsorption is pH dependent. In the range from pH 6 to 8, highest adsorbent loadings were achieved for pH 6. Adsorption efficiency decreases for higher values of pH.

- Chromate adsorption is water matrix dependent. Adsorbent loadings achieved in DI water were higher than in DW. In DW water the adsorption is not efficient, the maximum capacity value reached was 1.65 mg/g Cr. Interfering effect of competitor ions like sulfate, chloride or silicate could be the cause.

- Chromate adsorption was less efficient than phosphate adsorption, thus achieved loadings were lower.

- High concentration of chromium (up to 50 mg/L) could be a source of error. Maximum capacities reached are not very high so the equilibrium concentration is still high.

- The extraction of GFH is an important step in the experimental work. GFH suspension must be shaking and every extraction should be from the same point to have the required concentration.

The following part of the study would be the analysis of adsorption kinetics of phosphate and chromium adsorption, with the influence of pH and water matrix, to study the increase of the loading with time.

The achieved adsorbent loadings for phosphate were higher for every case than for chromate adsorption. Studying the competition of phosphate and chromate in the adsorption onto GFH could be also a following step. Another aspect to research would be the chromium adsorption in Berlin DW, with very low achieved capacities. Analyzing the possible effects, which ions could be part of the interfering effect in the adsorption.

It would be also interesting to research about an improvement in the GFH properties, trying to obtain a better efficiency in chromate adsorption.

6. Nomenclature

AAS	Atom adsorption spectometry	-
Agg	agglomerates	-
BES	N,N-Bis(2-hydroxyethyl)-2-aminoethanesulfonic Acid	-
c0	initial concentration	g/L
c_{eq}	Equilibrium adsorbate concentration	g/L
Cr	Chromium	-
DI	De-ionized Water	-
DNA	Desoxyribonucleic Acid	-
DW	Drinking Water	-
FIA	Flow injection analysis	-
GFH	Granular ferric hydroxide	-
IC	Ionic chromatography	-
K_F	Freundlich isotherm coefficient	$(L/g)^n$
K_L	liquid-phase mass transfer coefficient	m/t
m_a	adsorbent mass	g
MES	2-(N-morpholino)ethanesulfonic Acid	-
n	Freundlich isotherm exponent	-
P	Phosphorus	-
pH_{pzc}	pH point of zero charge	-
q_{eq}	Adsorbed concentration	g/g
q_{max}	maximum adsorbed concentration	g/g
T	Temperature	°C
TAPS	(N-Tris(hydroxymethyl)methyl-3-aminopropanesulfonic Acid	-
V_L	volume of adsorbate solution	L

7. Bibliography

Asgari, A. R. *et al.* (2008) 'Removal of Hexavalent Chromium from Drinking Water by Granular Ferric Hydroxide', *Iran. J. Environ. Health. Sci. Eng.*, Vol. 5(No. 4), pp. 277–282.

Back, C. (2012) 'PinAAcle 900 Geräte Handbuch', pp. 3–4.

Bahr, C. (2012) 'Entfernung von Uran aus Trinkwasser durch Adsorption an Granuliertem Eisenhydroxid (GEH)', p. 244.

Biotech, A. P. (1991) 'Chromatography Ion Exchange Chromatography', *Ion Exchange Chromatography: Principles and Methods*, pp. 9–154. doi: 10.1002/0471140864.ps0802s15.

Dale, I. M. (1982) 'Atomic Absorption Spectrometry', *Techniques and Instrumentation in Analytical Chemistry*, 5, pp. 381–394. doi: 10.1016/S0167-9244(08)70094-5.

Kikas, T. (2014) 'Introduction to Flow Injection Analysis (FIA) Determination of Chloride Ion Concentration'. Available at: ww2.chemistry.gatech.edu/class/analyt/fia.pdf.

L. Sigg und W. Stumm (1996) 'Eine Einführung in die Chemie wässriger Lösungen und natürlicher Gewässer', *vdf Hochschulverlag AG an der ETH Zürich und B.G. Teubner Stuttgart*.

Lazaridis, N. K. (2004) 'Chromium(VI) sorptive removal from aqueous solutions by nanocrystalline akaganèite', *Chemosphere*, 58, pp. 65–73.

Rabah, F. (2015) 'Water Treatment'.

Sperlich, A. (2010) 'Phosphate adsorption onto granular ferric hydroxide (GFH) for wastewater reuse'.

Technion, I. I. of T. (2017) 'Removal of inorganic contaminants form aqueous solutions by novel hybrid adsorption/filtration processes', *Rabin Desalination Laboratory*.

Worch, E. (2014) 'Adsorption Technology in Water Treatment', pp. 8–11.

X.-H. Guan, J. W. und C. C. C. (2007) 'Removal of arsenic from water using granular ferric hydroxide: Macroscopic and microscopic studies', *Journal of Hazardous Materials*, pp. 178–185.

Zelmanov, G. and Semiat, R. (2011) 'Iron (Fe +3) oxide/hydroxide nanoparticles-based agglomerates suspension as adsorbent for chromium (Cr +6) removal from water and recovery', *Separation and Purification Technology*. Elsevier B.V., 80(2), pp. 330–337. doi: 10.1016/j.seppur.2011.05.016.

Zelmanov, G. and Semiat, R. (2015) 'The influence of competitive inorganic ions on phosphate removal from water by adsorption on iron (Fe^{+3}) oxide/hydroxide nanoparticles-based agglomerates', *Journal of Water Process Engineering*. Elsevier Ltd, 5, pp. 143–152. doi: 10.1016/j.jwpe.2014.06.008.

8. List of figures

9. List of tables

10. Appendix

Tables

Tables of the batch adsorption isotherms are attached in this part. All the values and conditions needed to perform the experiments of phosphate and chromate adsorption onto GFH and agglomerates.

Sample	Solution[L]	TAPS [mmol/L]	MGEH[g]	CGEH[mg/L]	c0 (P) [mg/L]	c* (P) [mg/L]	q [mg/g P]	Contact time [h]
P0	0,2	2	0	0	4	4,1422	-	96
PP0	0,2	2	0	0	4	3,913	-	96
P1	0,2	2	0,016	80	4	2,989	12,9825	96
PP1	0,2	2	0,016	80	4	3,081	11,8325	96
P2	0,2	2	0,0252	126	4	2,578	11,5047619	96
PP2	0,2	2	0,0252	126	4	2,513	12,02063492	96
P3	0,2	2	0,0344	172	4	1,987	11,86395349	96
PP3	0,2	2	0,0344	172	4	2,064	11,41627907	96
P4	0,2	2	0,0436	218	4	1,726	10,55779817	96
PP4	0,2	2	0,0436	218	4	1,707	10,64495413	96
P5	0,2	2	0,0528	264	4	1,322	10,24848485	96
PP5	0,2	2	0,0528	264	4	1,059	11,24469697	96
P6	0,2	2	0,062	310	4	0,936	9,972903226	96
PP6	0,2	2	0,062	310	4	0,85	10,25032258	96
P7	0,2	2	0,0712	356	4	0,603	9,619662921	96
PP7	0,2	2	0,0712	356	4	0,635	9,529775281	96
P8	0,2	2	0,0792	396	4	0,373	9,228787879	96
PP8	0,2	2	0,0792	396	4	0,435	9,072222222	96

Table 10.1: Batch phosphate adsorption experiment in DI water at pH 8.

Sample	Solution[L]	TAPS [mmol/L]	MGEH[g]	CGEH[mg/L]	c0 (P) [mg/L]	c* (P) [mg/L]	q [mg/g P]	Contact time [h]
P0	0,2	2	0	0	4	3,642	-	96
PP0	0,2	2	0	0	4	3,787	-	96
P1	0,2	2	0,016	80	4	2,778	11,70625	96
PP1	0,2	2	0,016	80	4	2,78	11,68125	96
P2	0,2	2	0,0252	126	4	2,112	12,71825397	96
PP2	0,2	2	0,0252	126	4	2,258	11,55952381	96
P3	0,2	2	0,0344	172	4	1,678	11,84011628	96
PP3	0,2	2	0,0344	172	4	1,563	12,50872093	96
P4	0,2	2	0,0528	264	4	0,886	10,71401515	96
PP4	0,2	2	0,0528	264	4	0,888	10,70643939	96
P5	0,2	2	0,062	310	4	0,637	9,927419355	96
P6	0,2	2	0,062	310	4	0,532	10,26612903	96
P7	0,2	2	0,0804	402	4	0,208	8,722636816	96
PP7	0,2	2	0,0804	402	4	0,24	8,643034826	96
P8	0,2	2	0,09	450	4	0,175	7,865555556	96
PP8	0,2	2	0,09	450	4	0,175	7,865555556	96
P9	0,2	2	0,1	500	4	0,103	7,223	96
PP9	0,2	2	0,1	500	4	0,086	7,257	96

Table 10.2: Batch phosphate adsorption experiment in DI water with 10 mmol/L NaCl at pH 8.

Sample	Solution[L]	BES [mmol/L]	MGEH[g]	CGEH[mg/L]	c0 (P) [mg/L]	c* (P) [mg/L]	q [mg/g P]	Contact time [h]
P0	0,2	2	0	0	4	4,156	-	96
PP0	0,2	2	0	0	4	4,129	-	96
P1	0,2	2	0,008	40	4	3,391	18,7875	96
PP1	0,2	2	0,008	40	4	3,426	17,9125	96
P2	0,2	2	0,019	95	4	2,839	13,72105263	96
PP2	0,2	2	0,019	95	4	2,522	17,05789474	96
P3	0,2	2	0,03	150	4	1,737	16,03666667	96
PP3	0,2	2	0,03	150	4	1,666	16,51	96
P4	0,2	2	0,052	260	4	0,403	14,38269231	96
PP4	0,2	2	0,052	260	4	0,455	14,18269231	96
P5	0,2	2	0,063	315	4	0,203	12,50634921	96
P6	0,2	2	0,074	370	4	0,075	10,99324324	96
P7	0,2	2	0,082	410	4	0,041	10,00365854	96
PP7	0,2	2	0,082	410	4	0,047	9,98902439	96
P8	0,2	2	0,092	460	4	0,028	8,944565217	96
PP8	0,2	2	0,092	460	4	0,027	8,94673913	96

Table 10.3: Batch phosphate adsorption experiment in DI water with 10 mmol/L NaCl at pH 7.

Sample	Solution[L]	MES [mmol/L]	MGEH[g]	CGEH[mg/L]	c0 (P) [mg/L]	c* (P) [mg/L]	q [mg/g P]	Contact time [h]
P0	0,2	2	0	0	4	4,065	-	96
PP0	0,2	2	0	0	4	4,608	-	96
P1	0,2	2	0,008	40	4	3,447	22,2375	96
PP1	0,2	2	0,008	40	4	3,632	17,6125	96
P2	0,2	2	0,018	90	4	2,175	24,01666667	96
PP2	0,2	2	0,018	90	4	2,256	23,11666667	96
P3	0,2	2	0,028	140	4	1,355	21,29642857	96
PP3	0,2	2	0,028	140	4	1,296	21,71785714	96
P4	0,2	2	0,048	240	4	0,209	17,19791667	96
PP4	0,2	2	0,048	240	4	0,218	17,16041667	96
P5	0,2	2	0,058	290	4	0,08	14,67758621	96
PP5	0,2	2	0,058	290	4	0,052	14,77413793	96
P6	0,2	2	0,078	390	4	0,017	11,07564103	96
PP6	0,2	2	0,078	390	4	0,016	11,07820513	96
P7	0,2	2	0,086	430	4	0,014	10,05232558	96
PP7	0,2	2	0,086	430	4	0,014	10,05232558	96
P8	0,2	2	0,096	480	4	0,012	9,009375	96
PP8	0,2	2	0,096	480	4	0,012	9,009375	96

Table 10.4: Batch phosphate adsorption experiment in DI water with 10 mmol/L NaCl at pH 6.

Sample	Solution[L]	BES [mmol/L]	MGEH[g]	CGEH[mg/L]	c0 (P) [mg/L]	c* (P) [mg/L]	q [mg/g P]	Contact time [h]
P0	0,2	2	0	0	4	3,89	-	96
PP0	0,2	2	0	0	4	3,91	-	96
P1	0,2	2	0,008	40	4	2,9	25	96
PP1	0,2	2	0,008	40	4	3	22,5	96
P2	0,2	2	0,018	90	4	1,86	22,66666667	96
PP2	0,2	2	0,018	90	4	1,77	23,66666667	96
P3	0,2	2	0,028	140	4	1,042	20,41428571	96
PP3	0,2	2	0,028	140	4	1,011	20,63571429	96
P4	0,2	2	0,048	240	4	0,226	15,30833333	96
PP4	0,2	2	0,048	240	4	0,197	15,42916667	96
P5	0,2	2	0,058	290	4	0,116	13,04827586	96
PP5	0,2	2	0,058	290	4	0,116	13,04827586	96
P6	0,2	2	0,078	390	4	0,071	9,817948718	96
PP6	0,2	2	0,078	390	4	0,077	9,802564103	96
P7	0,2	2	0,086	430	4	0,047	8,960465116	96
PP7	0,2	2	0,086	430	4	0,053	8,946511628	96
P8	0,2	2	0,096	480	4	0,053	8,014583333	96
PP8	0,2	2	0,096	480	4	0,041	8,039583333	96

Table 10.5: Batch phosphate adsorption experiment in Berlin DW at pH 7.

Sample	Solution[L]	TAPS [mmol/L]	MGEH[g]	CGEH[g/L]	c0 (Cr) [mg/L]	c* (Cr) [mg/L]	q [mg/g P]	Contact time [h]
P1	0,2	2	0,1	0,5	0,25	0,10627	0,28746	24
PP1	0,2	2	0,1	0,5	0,25	0,09889	0,30222	24
P2	0,2	2	0,1	0,5	0,5	0,19945	0,6011	24
PP2	0,2	2	0,1	0,5	0,5	0,204515	0,59097	24
P3	0,2	2	0,1	0,5	1	0,479285	1,04143	24
PP3	0,2	2	0,1	0,5	1	0,47154	1,05692	24
P4	0,2	2	0,1	0,5	1,5	0,73601	1,52798	24
PP4	0,2	2	0,1	0,5	1,5	0,75695	1,4861	24
P5	0,2	2	0,1	0,5	2	1,11074	1,77852	24
PP5	0,2	2	0,1	0,5	2	1,14642	1,70716	24
P5	0,2	2	0,1	0,5	3	1,74584	2,50832	24
PP5	0,2	2	0,1	0,5	3	1,72384	2,55232	24
P6	0,2	2	0,1	0,5	4	2,52615	2,9477	24
PP6	0,2	2	0,1	0,5	4	2,5144	2,9712	24

Table 10.6: Batch chromate adsorption experiment in DI water at pH 8.

Sample	Solution[L]	BES [mmol/L]	MGEH[g]	CGEH[g/L]	c0 (Cr) [mg/L]	c* (Cr) [mg/L]	q [mg/g P]	Contact time [h]
P1	0,2	2	0,1	0,5	0,25	0,014362	0,471276	24
PP1	0,2	2	0,1	0,5	0,25	0,013834	0,472332	24
P2	0,2	2	0,1	0,5	0,5	0,031998	0,936004	24
PP2	0,2	2	0,1	0,5	0,5	0,030304	0,939392	24
P3	0,2	2	0,1	0,5	1	0,08544	1,82912	24
PP3	0,2	2	0,1	0,5	1	0,078445	1,84311	24
P4	0,2	2	0,1	0,5	1,5	0,15002	2,69996	24
PP4	0,2	2	0,1	0,5	1,5	0,140915	2,71817	24
P5	0,2	2	0,1	0,5	2	0,235605	3,52879	24
PP5	0,2	2	0,1	0,5	2	0,238515	3,52297	24
P6	0,2	2	0,1	0,5	3	0,44441	5,11118	24
PP6	0,2	2	0,1	0,5	3	0,465745	5,06851	24

Table 10.7: Batch chromate adsorption experiment in DI water at pH 7.

Sample	Solution[L]	MES [mmol/L]	MGEH[g]	CGEH[g/L]	c0 (Cr) [mg/L]	c* (Cr) [mg/L]	q [mg/g P]	Contact time [h]
P1	0,2	2	0,1	0,5	0,25	0,002307	0,495386	24
PP1	0,2	2	0,1	0,5	0,25	0,002156	0,495688	24
P2	0,2	2	0,1	0,5	0,5	0,004229	0,991542	24
PP2	0,2	2	0,1	0,5	0,5	0,004289	0,991422	24
P3	0,2	2	0,1	0,5	1	0,01025	1,9795	24
PP3	0,2	2	0,1	0,5	1	0,013185	1,97363	24
P4	0,2	2	0,1	0,5	1,5	0,025385	2,94923	24
PP4	0,2	2	0,1	0,5	1,5	0,024235	2,95153	24
P5	0,2	2	0,1	0,5	2	0,03542	3,92916	24
PP5	0,2	2	0,1	0,5	2	0,03732	3,92536	24
P6	0,2	2	0,1	0,5	3	0,10663	5,78674	24
PP6	0,2	2	0,1	0,5	3	0,105845	5,78831	24
P7	0,2	2	0,1	0,5	4	0,21975	7,5605	24
PP7	0,2	2	0,1	0,5	4	0,21986	7,56028	24

Table 10.8: Batch chromate adsorption experiment in DI water at pH 6.

Sample	Solution[L]	BES [mmol/L]	MGEH[g]	CGEH[g/L]	c0 (Cr) [mg/L]	c* (Cr) [mg/L]	q [mg/g P]	Contact time [h]
P1	0,2	2	0,1	0,5	0,25	0,017743	0,464514	24
PP1	0,2	2	0,1	0,5	0,25	0,015682	0,468636	24
P2	0,2	2	0,1	0,5	0,5	0,035887	0,928226	24
PP2	0,2	2	0,1	0,5	0,5	0,038828	0,922344	24
P3	0,2	2	0,1	0,5	1	0,094115	1,81177	24
PP3	0,2	2	0,1	0,5	1	0,09459	1,81082	24
P4	0,2	2	0,1	0,5	1,5	0,17684	2,64632	24
PP4	0,2	2	0,1	0,5	1,5	0,152635	2,69473	24
P5	0,2	2	0,1	0,5	2	0,25055	3,4989	24
PP5	0,2	2	0,1	0,5	2	0,280565	3,43887	24
P5	0,2	2	0,1	0,5	3	0,57592	4,84816	24
PP5	0,2	2	0,1	0,5	3	0,506395	4,98721	24
P6	0,2	2	0,1	0,5	4	0,86585	6,2683	24
PP6	0,2	2	0,1	0,5	4	0,85413	6,29174	24

Table 10.9: Batch chromate adsorption experiment in DI water with 10 mmol/L NaCl at pH 7.

Sample	Solution[L]	BES [mmol/L]	MGEH[g]	CGEH[g/L]	c0 (Cr) [mg/L]	c* (Cr) [mg/L]	q [mg/g P]	Contact time [h]
P1	0,2	2	0,1	0,5	0,25	0,13805	0,2239	24
PP1	0,2	2	0,1	0,5	0,25	0,130985	0,23803	24
P2	0,2	2	0,1	0,5	0,5	0,284765	0,43047	24
PP2	0,2	2	0,1	0,5	0,5	0,27318	0,45364	24
P3	0,2	2	0,1	0,5	1	0,63826	0,72348	24
PP3	0,2	2	0,1	0,5	1	0,61631	0,76738	24
P4	0,2	2	0,1	0,5	1,5	1,0087	0,9826	24
PP4	0,2	2	0,1	0,5	1,5	1,03904	0,92192	24
P5	0,2	2	0,1	0,5	2	1,45912	1,08176	24
PP5	0,2	2	0,1	0,5	2	1,47174	1,05652	24
P5	0,2	2	0,1	0,5	3	2,3316	1,3368	24
PP5	0,2	2	0,1	0,5	3	2,2979	1,4042	24
P6	0,2	2	0,1	0,5	4	3,17085	1,6583	24
PP6	0,2	2	0,1	0,5	4	3,1787	1,6426	24

Table 10.10: Batch chromate adsorption experiment in Berlin DW at pH 7.

Sample	Solution[L]	MES [mmol/L]	MGEH[g]	CAgg[g/L]	c0 (P) [mg/L]	c* (P) [mg/L]	q [mg/g P]	Contact time [h]
P0	0,2	2	0	0	10	10,089651	-	96
PP0	0,2	2	0	0	10	10,136228	-	96
P1	0,2	2	0,4	2	1	0,048842	0,475579	96
PP1	0,2	2	0,4	2	1	0,009887	0,4950565	96
P2	0,2	2	0,4	2	2	0,007522	0,996239	96
PP2	0,2	2	0,4	2	2	0,006596	0,996702	96
P3	0,2	2	0,4	2	4	0,058028	1,970986	96
PP3	0,2	2	0,4	2	4	0,204282	1,897859	96
P4	0,2	2	0,4	2	6	1,269037	2,3654815	96
PP4	0,2	2	0,4	2	6	1,004035	2,4979825	96
P5	0,2	2	0,4	2	8	2,867571	2,5662145	96
PP5	0,2	2	0,4	2	8	2,346874	2,826563	96
P6	0,2	2	0,4	2	10	4,331567	2,8342165	96
PP6	0,2	2	0,4	2	10	3,947596	3,026202	96
P7	0,2	2	0,4	2	12	5,59442	3,20279	96
PP7	0,2	2	0,4	2	12	5,747943	3,1260285	96

Table 10.11: Batch phosphate adsorption experiment in DI water at pH 6.

Sample	Solution[L]	MES [mmol/L]	MGEH[g]	CAgg[g/L]	c0 (Cr) [mg/L]	c* (Cr) [mg/L]	q [mg/g P]	Contact time [h]
P0	0,2	2	0	0	50	45,65	-	96
PP0	0,2	2	0	0	50	45,44	-	96
P1	0,2	2	0,4	2	2	0,01007	0,994965	96
PP1	0,2	2	0,4	2	2	0,00981	0,995095	96
P2	0,2	2	0,4	2	4	0,03467	1,982665	96
PP2	0,2	2	0,4	2	4	0,03698	1,98151	96
P3	0,2	2	0,4	2	10	0,3	4,85	96
PP3	0,2	2	0,4	2	10	0,47	4,765	96
P4	0,2	2	0,4	2	15	1,71	6,645	96
PP4	0,2	2	0,4	2	15	2,13	6,435	96
P5	0,2	2	0,4	2	20	7,19	6,405	96
PP5	0,2	2	0,4	2	20	7,95	6,025	96
P6	0,2	2	0,4	2	30	14,47	7,765	96
PP6	0,2	2	0,4	2	30	13,43	8,285	96
P7	0,2	2	0,4	2	50	31,25	9,375	96
PP7	0,2	2	0,4	2	50	30,6	9,7	96

Table 10.12: Batch chromate adsorption experiment in DI water at pH 6.